STRESS EFFECT ON CREEP RATES OF A FROZEN CLAY SOIL FROM THE STANDPOINT OF RATE PROCESS THEORY

Thesis for the Degree of Ph. D. MICHIGAN STATE UNIVERSITY
Waddah Akili
1966



This is to certify that the

thesis entitled

STRESS EFFECT ON CREEP RATES OF A FROZEN CLAY SOIL FROM THE STANDPOINT OF RATE PROCESS THEORY

presented by

Waddah Akili

has been accepted towards fulfillment of the requirements for

Ph. D. degree in Civil Engineering

Major professor

Date Dec. 30, 1965

ABSTRACT

STRESS EFFECT ON CREEP RATES OF A FROZEN CLAY SOIL FROM THE STANDPOINT OF RATE PROCESS THEORY

By Waddah Akili

The effect of stress on the creep rate of a frozen clay soil has been approached in the light of the rate process theory. Experimental creep data were obtained from duplicate frozen specimens of remolded clay crept over a range of stresses and temperatures. Stress reduction techniques were employed to determine the stress effect on the creep rate under constant structure conditions.

The rate equation of the form $\dot{\xi} = K \sinh B \vec{O}$, where $\dot{\xi}$ is the axial strain rate and \vec{O} is the axial stress, was replaced by $\dot{\xi} = \frac{K}{2} e^{\vec{B} \vec{O}}$ for the relatively high stresses investigated. Experimental results show how the parameters B and K vary with the stress at the several temperatures investigated. For high stresses and a given temperature, B remains reasonably constant. For lower stresses (below the critical stress), B increases with decreasing applied stress. The variation in B (equals $\frac{\sqrt{2}}{3} \frac{qA \ell}{2kT}$) is attributed to the change in flow volume (qA ℓ). The computed flow volume indicates that creep behavior is controlled at the particle and/or ice contact points. The variation of the parameter K (equals to S $e^{-\Delta F/RT}$)

appears to be related primarily to changes in the magnitude of the free energy of activation (ΔF). An observed ΔF equal to about 100 k cal/mole was obtained for higher stresses (above the critical stress) at temperatures below -9°C. Larger values of ΔF obtained at lower stresses and warmer temperatures may be fictitious. The structure term S involves stress and temperature history plus the instantaneous values of applied stress and strain.

The division of creep into the damped and undamped regions by the critical stress was substantiated by test data. The estimated critical stress corresponds to a creep rate of about 10⁻⁴ in/in/minute.

The varying stress-constant time method was applied on regular creep curves obtained concurrently with stress reduction data. The results of this method supported earlier observations regarding the separation of creep by the critical stress into the damped and undamped regions.

A method is shown whereby present data may be extrapolated over a wider range of stresses and temperatures.

STRESS EFFECT ON CREEP RATES OF A FROZEN CLAY SOIL FROM THE STANDPOINT OF RATE PROCESS THEORY

By

Waddah Akili

A THESIS

Submitted to
Michigan State University
in partial fulfillment of the requirements
for the degree of

DOCTOR OF PHILOSOPHY

Department of Civil Engineering

ACKNOWLEDGEMENTS

The writer wishes to express his deep appreciation to his thesis advisor, Dr. O. B. Andersland, Associate Professor of Civil Engineering, for his help and guidance. Thanks are also due the other members of the writer's doctoral committee: Dr. L. E. Malvern, Professor of Applied Mechanics, Dr. C. P. Wells, Professor and Chairman of the Department of Mathematics, and Dr. T. H. Wu, Professor of Civil Engineering, who is presently at Ohio State University. The writer is indebted to his colleague, H. B. Dillon, for his assistance in the laboratory.

Thanks go to the National Science Foundation and the Division of Engineering Research at Michigan State University for the financial assistance that made this study possible.

TABLE OF CONTENTS

CHAPTER		PAGE
I.	INTRODUCTION	1
II.	REVIEW AND THEORY	4
	General Description	4
	Structure of Frozen Soils	6
	Deformation Aspects of Frozen Soils	9
	Development of the Rate Process Equation	11
	Application of the Rate Process Theory to Creep of Frozen Soils	20
III.	EXPERIMENTAL TECHNIQUES	25
	Stress Reduction Method	25
	Successive Stress Reductions Method	26
	Varying Stress-Constant Strain Method	26
	Varying Stress-Constant Time Method	28
	Comparison of Various Techniques	28
IV.	EXPERIMENTAL PROGRAM	32
	Soil Studied	32
	Sample Preparation	35
	Test Setup	36
	Sample Loading and Unloading	38
v.	EXPERIMENTAL RESULTS	43
	Single Stress Reduction	43
	Successive Stress Reductions	46
	Regular Creep	48
	The Effect of Stress History on the B and K Parameters	48
VI.	DISCUSSION	64
	General	64
	The B Parameter	70
	The K Parameter	75
VII.	SUMMARY AND CONCLUSION	84
BIBLIOGRA	PHY	87
APPENDIX		90

LIST OF TABLES

TABLE		PAGE
4-1	Index Properties of Sault St. Marie Clay	31
4-2	Molded Moisture Contents and Average Dry Density of Soil Cakes (Sault St. Marie Clay)	36
5-1	Summary of Creep Data on the Sault St. Marie Clay Using Single Stress Reduction (Temperature -12°C)	61
5-2	Summary of Creep Data on the Sault St. Marie Clay Using Successive Stress Reductions at Several Temperatures	62
6-1	Summary of Data on the Duration of Test Method for Determination of the Free Energy of Activation Under a Creep Stress of 675 psi (Frozen Sault St. Marie Clay)	79

LIST OF FIGURES

FIGURE		PAGE
2-1	Typical Creep Curves for Frozen Soils	5
2-2	Distribution of Soil Water After Freezing in a Closed System (After Jackson and Chalmers, 1957).	7
2-3	Energy Change of a System During the Course of a Reaction	13
2-4	Modified Energy Map Upon Application of a Shearing Stress	14
2-5	Distance that Flow Units Move in Direction of Strain and Distances Between Flow Units	15
3-1	Varying Stress-Constant Strain Method	27
3-2	Varying Stress-Constant Time Method	28
4-1	Grain Size Distribution Curve for Sault St. Marie Clay	33
4-2	Unfrozen Water Content - Sault St. Marie Clay (After Dillon, in preparation)	34
4-3	Temperature Measuring Equipment	39
4-4	Triaxial Cell and Test Specimens	39
4-5	Schematic Diagram of the Constant Temperature Stress Reduction Setup	41
5-1	Typical Examples of the Effect of Single Stress Reduction on Creep Rate - Sault St. Marie Clay	50
5-2	Effect of True Stress on Creep Rate Using Single Stress Reduction - Sault St. Marie Clay	51

FIGURE		PAGE
5-3	Typical Example of the Effect of Successive Stress Reductions on Creep Rate - Sault St. Marie Clay	52
5-4	Effect of True Stress on Creep Rate - Sault St. Marie Clay	53
5-5	Initial Portion of Creep Curves at Several Stresses and Constant Temperature - Sault St. Marie Clay	54
5-6	Creep Curves at Several Stresses and Constant Temperature	55
5-7a	Stress-Strain History Influence on B and K Parameters - Sample A-3 (1)	56
5-7b	Stress-Strain History Influence on B and K Parameters - Sample A-3 (10)	57
5-7c	Stress-Strain History Influence on B and K Parameters - Sample A-3 (6)	58
5-7d	Stress-Strain History Influence on B and K Parameters - Sample A-3 (14)	59
5-7e	Stress-Strain History Influence on B and K Parameters - Sample A-3 (15)	60
6-1	Schematic Diagram Showing the Change in Strength of a Frozen Clay Soil with Time	66
6-2	Stress-Strain Curves Derived from Creep Tests for Selected Times	68
6-3	Creep Rate-Stress Relationship at Constant Times (t ₁ = 5 min.; t ₂ = 10 min.; t ₃ = 15 min.)	68
6-4	Axial Stress Versus Temperature for Selected Creep Rates	69
6-5	Variation of B Parameter with Temperature at Constant Creep Rates	73

FIGURE		PAGE
6-6	Simplified Representation of Contact Region Between Two Particles and Adjacent Ice Grains	72
6-7	The Creep Rate Temperature Relationship at Constant Stress	81
6-8	Creep Behavior of Frozen Sault St. Marie Clay - Evaluation of the Free Energy of Activation (ΔF) at 9 Per Cent Conventional Strain	82
6-9	Variation of Observed Free Energy of Activation with Axial Stress	83

NOTATION

A = area of flow unit in the shear plane

B = rate theory parameter equal to $\frac{\sqrt{2}}{3}$ $\frac{qA \ell}{2kT}$

C = a constant

 ΔF = free energy of activation per mole

 ΔH = the heat of activation per mole

h = Planck's constant = 6.626×10^{-27} ergs sec

k = Boltzmann's constant = 1.3805 x 10⁻¹⁶ ergs/°C/mole

k' = the specific rate of the process

K = rate theory parameter equal to $Se^{-\Delta F/RT}$

distance through which the shear stress acts in carrying the unit of flow from the initial to the final state

m = a "transmission coefficient," assumed to be unity

q = a stress concentration factor

R = gas constant = 1.987 cal per mole per degree C

S = a structure term, sensitive to stress history, temperature history, and the instantaneous values of stress and strain

 ΔS = the entropy of activation per mole

T = absolute temperature

t = time

 V_f = flow volume equal to qA p

T = the microscopic shear strain rate

 γ_{oct} = octahedral shear strain rate

€ = axial strain

 ϵ_{I} , ϵ_{II} , ϵ_{III} = principal strains

• = axial strain rate

 $\dot{\epsilon}_1$, $\dot{\epsilon}_2$, $\dot{\epsilon}_3$ = decreasing values of axial strain rate

 $\Delta \dot{\epsilon}$ = change in strain rate due to change in deviator stress

the distance the flow unit, or activated complex, moves in the direction of flow

λ₁ = the distance between flow units normal to the direction of flow

 $\lambda_2 \lambda_3$ = the effective cross-sectional area of the flow unit in the direction of applied stress

CI, CII, CIII = principal stresses

 $C = (C_1 - CIII) = principal stress difference or deviator stress$

 C_1 , C_2 , C_3 = decreasing order of deviator stress

 $\Delta C_1, \Delta C_2, \Delta C_3$ = decrements or increments in deviator stress

C_c = the critical stress which divides creep of frozen soils into damped and undamped regions

 \mathcal{T} = applied shear stress on the flow unit

 T_{oct} = octahedral shear stress

CHAPTER I

INTRODUCTION

The phenomenon of creep has been one of the major subjects of research for a variety of materials in the past decade. Scientists and engineers alike have explored the theoretical and experimental aspects of creep in search of a satisfactory general theory, but unfortunately no such theory has been developed as yet (Kennedy, 1963). Perhaps one source of the failure to uncover an adequate theory arises from the fact that practically all theories disregard the fact that material structure changes during creep (Dorn, 1954).

During the process of search for a theory, considerable progress has been made in understanding creep behavior. Many of these advances are primarily related to crystalline materials and particularly to metals. The early work on creep was dominated by the model concepts which are manifested in the great variety of empirical formulations. In the light of modern knowledge of crystal physics and material science, more emphasis has been placed on the microscopic aspects of creep and its constituent processes, particularly those that may be rate-determining.

One of the theories that reduce flow processes to the molecular level is the rate process theory (Glasstone, Laidler and Eyring, 1941).

Its application to a large number of materials such as ceramics, metals, rubber, asphalt, concrete and unfrozen soil has met with considerable success. (Kauzmann, 1941; Herrin and Jones, 1963; Mitchell, 1963). The theory explains macroscopic deformation in terms of the microscopic processes, and relates the rate of shear of a material to the applied shear stress, temperature and some basic properties of the material.

The phase composition of frozen soils (solid, liquid and gaseous matter) presents problems during the deformation process.

Structural changes in frozen soils during creep involve quantitative and qualitative changes. The amount of unfrozen water, the amount of ice in the frozen mass, the geometrical orientation of particles, and the mechanical properties of the ice are undergoing continuous change during creep (Tsytovich, 1963). These changes in structure complicate the creep process and hinder direct experimental analysis of conventional creep curves. Therefore, special experimental techniques must be employed to measure the effects of stress on creep rate under conditions of constant structures.

In this study the effect of stress on the creep rate of frozen soils has been approached in the light of rate process theory.

Variables such as molded dry density and molded water content were excluded as much as possible. Data have been obtained using the stress reduction method. Deformation-time curves obtained concurrently with the above data were used to compare results by

varying stress-constant time method.

Experimental results show how the parameters in the basic rate equation vary with stress at the several temperatures used.

Changes in flow volume appear to be related primarily to changes in contact area in regions of high stress concentration. An observed free energy of activation equal to 100 k cal/mole appears to remain reasonably constant in the undamped creep region at high stresses and temperatures below -9°C. Additional information was obtained on long term strength and a method whereby limited creep data may be extrapolated over a wider range of stresses and temperatures.

CHAPTER II

REVIEW AND THEORY

General Description

Frozen soils, like other deformable solids, exhibit timedependent deformation under stress. The essential features of creep
curves of frozen soils correspond to classical creep and may be
divided into several sections representing the various stages of
strain-time relation as illustrated schematically in the upper curve
of Figure 2-1. Stage 1, termed primary or transient creep,
represents the initial region of decreasing creep rate; Stage 2,
termed secondary or quasi-viscous flow, represents the region of
relatively constant creep rate; and finally, Stage 3, termed tertiary
or progressive creep, represents the region of increasing creep
rate leading eventually to failure. Tertiary creep may or may not
take place; instead deformation may proceed at an ever decreasing
rate. This depends on the magnitude of the applied stress and the
temperature of the frozen medium.

Creep curves of frozen soils may be divided, in general, into two categories, depending on the value of the creep stress (Vialov, 1961). If the stress does not exceed a certain limiting value, then the deformation is damped (damped creep) meaning that rate of deformation

decreases with time until it approaches zero. Thus, Stages 2 and 3 are missing in damped creep as illustrated in the lower curve of Figure 2-1. If the applied stress does exceed the limiting value, then the deformation is undamped (undamped creep), where the decelerating rate of deformation proceeds until a certain minimum rate is reached (depending on the magnitude of the applied stress) after which progressive flow takes place.

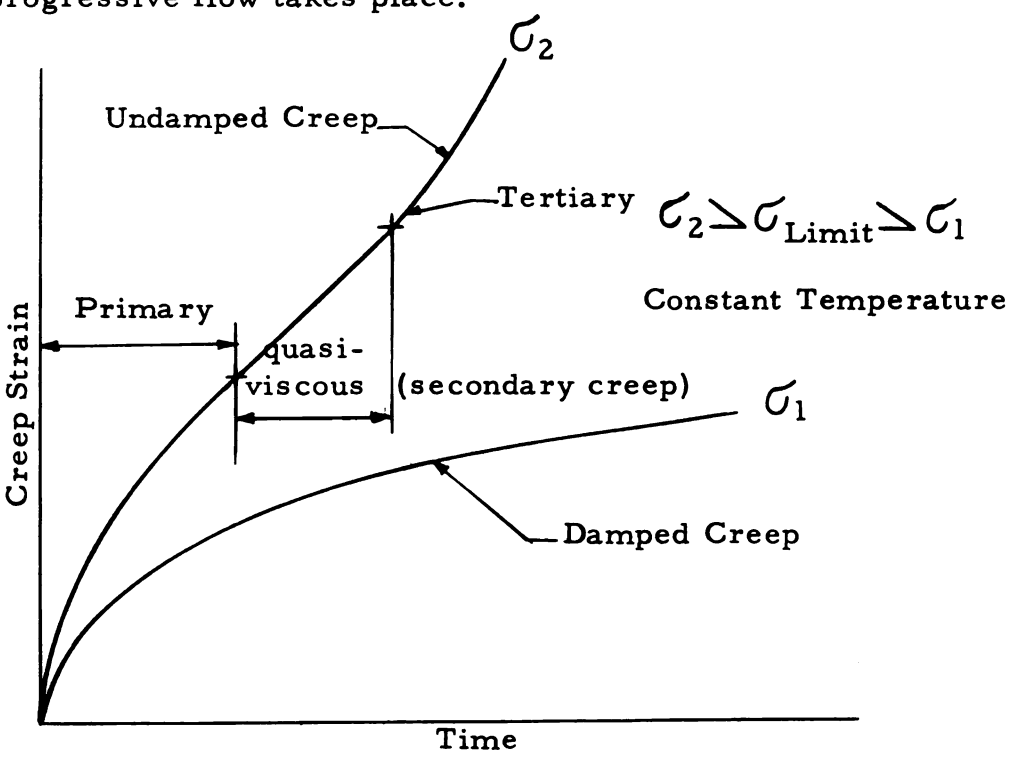


Figure 2-1. Typical Creep Curves for Frozen Soils

The division of the creep process into damped and undamped, the separation of the various stages of creep, and the duration of any one stage often depends on the precision of creep observations and the duration of such observations. The creep rate in the so-called steady

state region may slowly decrease if observed for long periods of time or on the contrary it may increase. How close is the creep rate in the steady state region to being a constant and the duration of the steady state depend primarily upon the applied stress (Vialov, 1961). The larger the stress, the shorter is the stage of steady state, and the faster is the transition into the tertiary stage.

Change in creep rate results from weakening and strengthening processes that operate simultaneously. If the process of strengthening is greater than that of weakening, the creep rate decreases (primary); if the two processes compensate one another, deformation proceeds at approximately a constant rate (steady state); and if the process of weakening is greater, then progressive flow (tertiary creep) begins leading to failure.

Structure of Frozen Soils

Frozen soil is an aggregated structure made up of soil grains, ice, unfrozen water and the gaseous phase (usually air). Properties of soil particles including size, shape and mineral composition have a significant effect on the frozen structure and its strength characteristics. The degree of packing of soil grains and their geometrical arrangement prior to freezing affect appreciably the void space in the soil mass and in turn the amount of frozen water. At low temperatures some unfrozen water remains at the clay mineral surface. The

relative thickness of this water film and the orientation of its molecules depend on the mineral type (Grim, 1953). During the process of freezing, particle reorientation takes place due to negative pore pressure that develops during the freezing process and also due to the slight volume changes caused by freezing of the free water in the soil mass (Broms and Yao, 1964). The freezing point of the free water in the soil decreases with decreasing average grain size of the soil. Ice forms in the large interstices (voids) before it forms in the minute channels within the soil mass. The ice formed is composed of many individual crystals and may be polycrystalline in nature.

The distribution of moisture in the soil after freezing depends on the direction of freezing, soil permeability and time. Tests conducted in a closed system by Jackson and Chalmers (1957), yielded results illustrated in Figure 2-2.

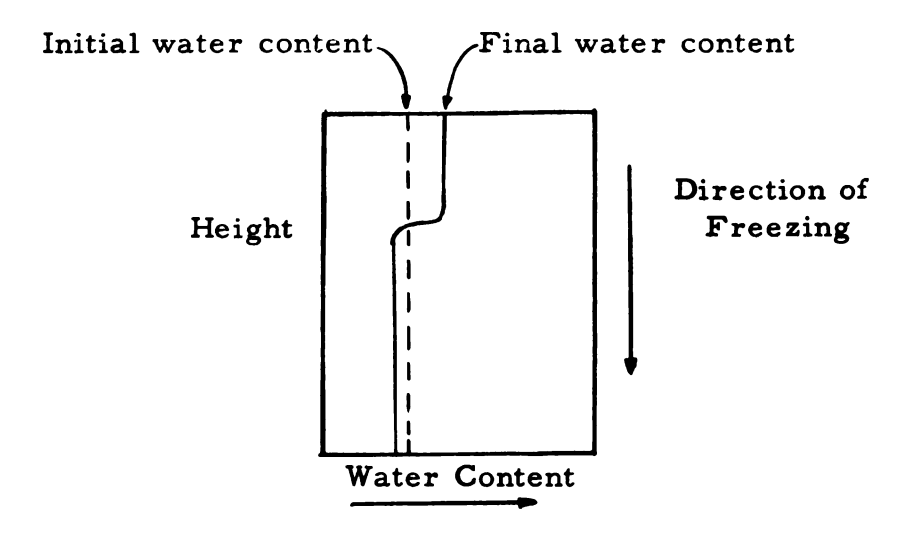


Figure 2-2. Distribution of Soil Water After Freezing in a Closed System (After Jackson and Chalmers, 1957).

Strength of the frozen soil may be considered as a function of bonding strength at particle to ice contacts, and at particle to particle contacts. The frozen mass may be thought of as a network of many contacts, where their strength and the total number of such contacts are necessarily a function of soil type, total amount of water present, temperature, and degree of packing of soil grains.

Particle to particle bond depends upon the molecular forces of attraction between mineral particles, which are separated by water films, the amount of such separation and the extent of the particle surfaces (Vialov, 1963; Lambe, 1960).

The soil-ice bond, which is believed to be the most important, depends upon the amount of ice, the area of contact and the temperature of the frozen soil. It is the least stable part of the bonding strength since it changes with any variation in temperature.

Reduction in temperature causes an increase in the amount of frozen water and in turn an increase in the soil-ice bonds. Such a change in temperature is accompanied also by a change in the mobility of hydrogen atoms in the ice crystalline lattice upon which the quality of ice depends (Tsytovich, 1963). Temperature reduction also causes a decrease in the thickness of liquid water films absorbed by the surface of ice crystals and significantly increases their strength, thus contributing to the overall strength of the frozen mass.

Deformation Aspects of Frozen Soils

Frozen soils may be considered as elasto-plasto-viscous bodies based on the deformation characteristics and the constituents of the frozen media (Vialov, 1961). The presence of frozen and unfrozen water in the frozen media presents problems of phase composition during the deformation process. Unlike other materials, frozen soils undergo drastic structural changes (ratio of frozen to unfrozen water) under the influence of stress. The dynamic equilibrium of ice and unfrozen water in frozen soils demands quantitative changes of unfrozen water and pore ice with any change of temperature and stress (Tsytovich, 1963). In other words, ice and unfrozen water strive to preserve the condition of equilibrium corresponding to a given stress and temperature.

The deformational resistance of frozen structure rests in the network of bonds formed at contact points. The strength of these bonds may vary widely as explained earlier, depending primarily on the temperature, amount of water present, and clay type. When external stresses are applied, some of these bonds will fail while others remain intact. This failure is due to plastic flow and melting of ice at areas of contact, weakening and leading to eventual break-up of bonds (Vialov, 1961). After breakage of bonds, ice crystals and mineral particles tend to reorient themselves with respect to the stress-axis. At the same time the unfrozen water, which increases

upon partial melting of the ice at the contacts, migrates from highly stressed zones to zones of lower stress where it refreezes. The movement of mineral particles and ice crystals away from the initial configuration results in new contacts and the formation of new bonds. New bonds will form also upon refreezing of the melted ice. Recrystallization of ice is accompanied by a reduction in the size of ice crystals and reorientation of such crystals into a favorable direction with the stress-axis. These latter changes occur rather slowly.

Thus, deformation of frozen soils under applied stress may be envisioned as the result of breaking and forming of bonds at contact points in the aggregated structure. It may be said that at the contact level interaction of solid units (particles, ice crystals) is involved. A useful analogy can be drawn from the phenomenon of sliding friction between solid surfaces, where shearing resistance develops by the interlocking asperities of the two surfaces brought together under the action of a normal force (Bowden and Tabor, 1954). Even in the case of highly polished ice surfaces, actual contact occurs over a very small area and the local stresses at the contact are sufficient to produce yielding.

Therefore, if the shearing force applied at the contact equals or exceeds the shearing strength of that contact, sliding will occur and the bonds in that contact will be broken. The ratio of shearing strength to shearing stress at a contact is not a constant, but depends upon the

speed of sliding (Burwell and Rabinowicz, 1953).

The deformation phenomenon, as viewed here, of contacts and shear forces acting at the contacts could provide a plausible explanation to the macroscopic aspects of deformation. However, to make use of the theoretical treatment of the rate process theory, the deformation process in frozen soils will be envisioned as movements of atoms and molecules rather than displacement at the contact level.

Development of the Rate Process Equation

According to the rate process theory (Glasstone, Laidler and Eyring, 1941), the rate of a reaction in a molecular process involves an exponential dependence on the temperature of the form:

Rate = $C e^{-E/kT}$ (2-1)

Where C = constant

E = energy supplied

k = Boltzmann's constant

T = absolute temperature

Rate process theory requires that molecules involved in the process must form an activated complex. The formation of an activated complex can be described as a process in which atoms in the molecules involved regroup themselves giving rise to a modified form of the initial state. This new configuration of atoms, although originated within the system of the initial substance and formed from the same

atoms, posesses different properties:

- (a) Its atoms are less densely packed and their motion is more disordered.
- (b) The strength of the interatomic bonds of the activated complex is lower than those in the initial state.
- (c) The activated complex has higher energy than the initial state (Osipov, 1964).

The formation of activated complexes requires energy. When this energy has been provided (either mechanically or thermally) from outside the system, the particular reaction goes to completion. A complex is regarded as being situated at the top of a free energy barrier lying between the initial and the final states. The course of a reaction may be represented by an energy map as shown in Figure 2-3. The points A and B correspond to initial and final equilibrium states, while point C represents the maximum energy level or the so-called energy barrier. Overcoming this barrier is a necessary condition for the activated complex to be formed. In passing from A to B, the energy increases, passing through its maximum C, and then decreases passing through the second minimum at point B. The elevation $\triangle H$ of point C above the level AB is termed the energy of activation or the heat of activation.

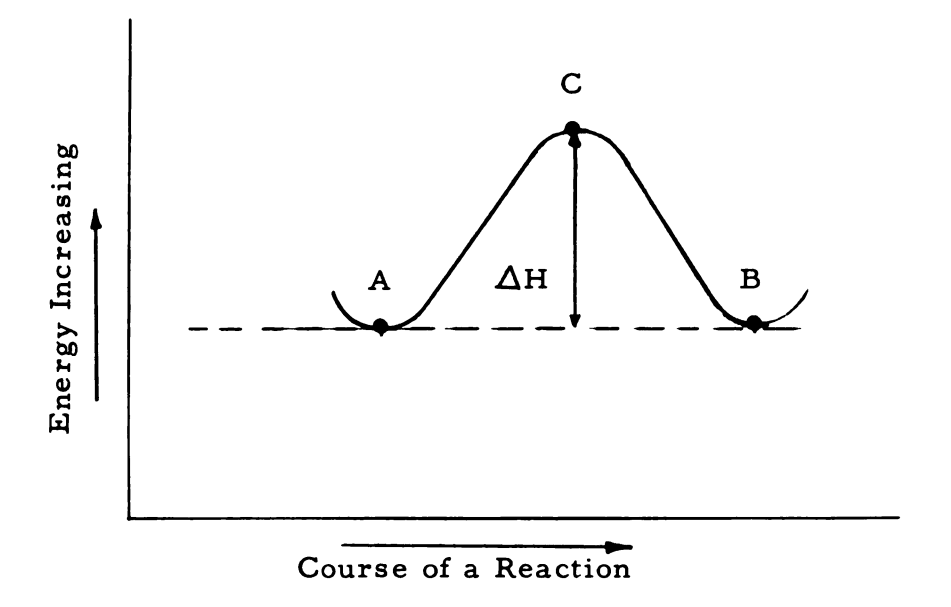


Figure 2-3. Energy Change of a System During the Course of a Reaction

It is generally recognized that all processes proceeding at a finite rate involve the formation of activated complexes (Osipov, 1964).

Flow processes reduced to the same molecular level, involve a similar movement as explained by the reaction rate theory (Glasstone, Laidler, and Eyring, 1941). Eyring's reaction rate equation of molecular processes based on the classical Maxwell-Boltzmann law of the distribution of energy in a system is:

$$k' = \frac{mkT}{h} e^{-\Delta F/RT}$$
 (2-2)

Where k' = the specific rate of the process

m = a "transmission coefficient", assumed to be unity

k = Boltzmann's constant = 1.3805 x 10⁻¹⁶ ergs/°C/mole

h = Planck's constant = 6.624×10^{-27} ergs sec

 ΔF = free energy of activation

R = the universal gas constant

T = the absolute temperature

In the development of the theory, it is assumed that flow takes place by movements of molecules or aggregates of molecules (flow units) into vacancies (holes) in the material, or by displacements of the vacancies themselves with the material (Herrin and Jones, 1963). Since the production of such vacancies by the movement of flow units requires that an energy barrier be overcome, the absolute rate relationship (Eq. 2-2) should be applicable to the evaluation of the rate of flow in a deformable material. Equation (2-2), however, was derived for equilibrium conditions.

In the case of an applied stress, Equation (2-2) must be appropriately modified. The energy added to the system due to the application of the shearing force, distorts the energy barrier. This distortion is additive on the ascending side of the energy barrier and subtractive on the descending portion as shown in Figure 2-4.

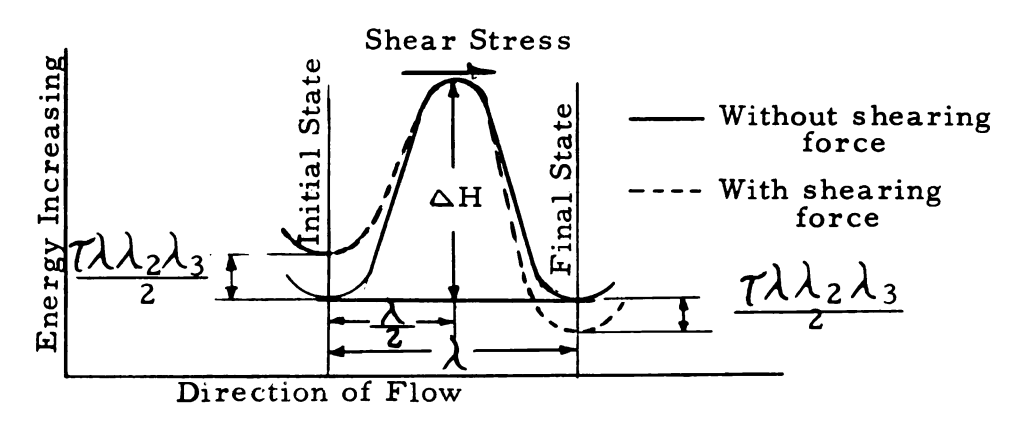


Figure 2-4. Modified Energy Map upon Application of a Shearing Stress

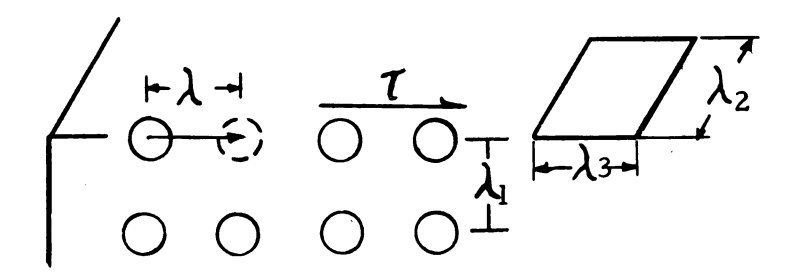


Figure 2-5. Distance that Flow Units Move in Direction of Strain and Distances Between Flow Units

The molecules (flow units) of the system may be arranged as shown in Figure 2-5,

Where T = the applied shear stress

\(\) = the distance the flow unit or activated complex moves in the direction of flow

λ₁ = the distance between flow units normal to the direction of flow

 $\lambda_2 \lambda_3$ = the effective cross-sectional area of the flow unit in the direction of applied stress

Since the force acting on a flow unit with cross-sectional area $\lambda_2\lambda_3$ is $7\lambda_2\lambda_3$, the amount of work done in moving the unit a distance λ is $7\lambda\lambda_2\lambda_3$. This is the work required to displace a flow unit from its initial state to its final state; i.e., the work the flow unit must do to overcome the potential barrier. However, for a symmetrical barrier, the state of higher energy is reached when the flow unit has moved a distance $\frac{\lambda}{2}$, and thus the amount of work required to surmount the energy barrier is $\frac{7\lambda\lambda_2\lambda_3}{2}$. After moving over the

peak of the barrier, it proceeds to its final state.

As a result of the applied stress on the flow unit, the energy barrier is altered by $\frac{7\lambda\lambda_2}{2}$ and the specific flow rate in the forward direction is given by

$$k' \exp\left(\frac{T\lambda\lambda_2\lambda_3}{2kT}\right)$$
 (2-3) (a)

and in the backward direction

$$k' \exp\left(-\frac{\tau \lambda \lambda_2 \lambda_3}{2kT}\right) \tag{2-3}$$

The net number of times any flow unit passes over the potential barrier is then

$$k' \left[\exp \left(\frac{\tau \lambda \lambda_2 \lambda_3}{2kT} \right) - \exp \left(-\frac{\tau \lambda \lambda_2 \lambda_3}{2kT} \right) \right]$$
 (2-4)

The net rate of flow in the forward direction resulting from the applied shearing stress (Υ) is the net specific rate of movement of the flow unit; i.e., the number of times per unit time that a flow unit moves forward over the energy barrier multiplied by the distance λ traversed per movement. Multiplying this value by $\frac{1}{\lambda_1}$ where λ_1 is the distance between flow units normal to the direction of flow gives, by definition, the rate of flow (Υ):

$$\dot{\gamma} = \frac{\lambda}{\lambda_1} k' \left[\exp \left(\frac{\tau \lambda \lambda_2 \lambda_3}{2kT} \right) - \exp \left(-\frac{\tau \lambda \lambda_2 \lambda_3}{2kT} \right) \right] (2-5)$$

which may be written as

$$\dot{\gamma} = \frac{2\lambda}{\lambda_1} \quad k' \sinh \frac{T\lambda \lambda_2 \lambda_3}{2kT}$$
 (2-6)

Since the applied stress on the flow unit is a shear stress, $\dot{\gamma}$ is then the rate of shearing strain.

Substituting equation (2-2) into (2-6) gives the shear strain rate

$$\dot{\gamma} = 2 \frac{\lambda}{\lambda_1} \frac{kT}{h} e^{-\frac{\Delta F}{RT}} \sinh \frac{\lambda \lambda_2 \lambda_3 \tau}{2kT}$$
 (2-7)

where the transmission coefficient(m) has been taken equal to unity.

The projected area of each flow unit in the shear plane is $A = \lambda_2 \lambda_3$, and the effective volume of the flow unit is $V_f = \lambda \lambda_2 \lambda_3 = qA\ell$, where q is a stress concentration factor.

Equation (2-7) can be written as:

$$\dot{\gamma} = 2 \frac{\lambda}{\lambda_1} \frac{kT}{h} e^{\Delta F/RT} \sinh \frac{qA \ell r}{2kT}$$
 (2-8)

It should be stated that V_f , which is a measure of the volume of the moving unit in the direction of force, should be a measure of the volume of vacancy (hole) created by the applied force. In order for flow units to move from one position of equilibrium to another, it is necessary that space be provided into which the units can move (Fredrickson and Eyring, 1948). Thus, the two volumes can be used interchangeably since they are of the same order of magnitude.

From thermodynamics, the free energy of activation (Δ F) may be written as a function of temperature:

$$\Delta \mathbf{F} = \Delta \mathbf{H} - \mathbf{T} \Delta \mathbf{S} \tag{2-9}$$

Where ΔH = the heat of activation

 ΔS = the entropy of activation

It is noted when $T=0^{\circ}k$, $\Delta F=\Delta H$. Hence, the heat of activation may be interpreted as being the energy which must be put into the system exclusive of thermal energy inherent in the system in order to bring about a reaction. However, the T ΔS term of the equation effectively represents the amount of thermal energy stored in the system due to its temperature. The free energy of activation (ΔF) is the amount of energy which must be added to the system to initiate a reaction.

Inserting equation (2-9) in equation (2-8) gives the following expression:

$$\dot{\gamma} = 2 \frac{\lambda}{\lambda_1} \frac{kT}{h} e^{-\Delta H/RT} e^{\Delta S/R} \sinh \frac{V_f \tau}{2kT}$$
 (2-10)

Herrin and Jones (1963) have indicated that λ and λ_1 are only approximations of the order of the size of a flow unit, and it may be assumed that $\frac{2\lambda}{\lambda_1} = 1$, with the result that:

$$\dot{\gamma} = \frac{kT}{h} e^{\Delta S/R} e^{-\Delta H/RT} \sinh \frac{V_f}{2kT} \mathcal{T}$$
 (2-11)

Equation (2-11) may be reduced to the form:

$$\dot{\gamma} = \dot{\gamma}_{o} \sinh \frac{\mathcal{T}}{\mathcal{T}_{o}}$$
Where $\frac{kT}{h} e^{\Delta S/R} e^{-\Delta H/RT} = \dot{\gamma}_{o}$
and $\frac{V_{f}}{2kT} = \frac{1}{\mathcal{T}_{o}}$

At constant temperatures $\dot{\gamma}_{o}$ and τ_{o} were found to be constants for certain materials. Herrin and Jones (1963) have shown

that $\dot{\gamma}_{\rm o}$ and $\mathcal{T}_{\rm o}$ are temperature-dependent terms for an asphalt material. Dorn and co-workers (1954) have shown that for polycrystalline aluminum the $\mathcal{T}_{\rm o}$ term is independent of temperature and stress and appears to be independent of the structure of the metal, while the $\dot{\gamma}_{\rm o}$ term is dependent on temperature, structure and stress.

Obviously, the $\dot{\gamma}_{\rm o}$ and $\mathcal{T}_{\rm o}$ terms in equation (2-12) are material dependent terms. For a given material their variation with external variables of stress and temperature can be determined experimentally.

This theory is quite general regarding the nature of the unit of flow and of the energy barrier restricting flow. The unit of flow can be an atom, a single molecule or a group of many molecules.

The barrier could arise directly from the repulsions between units of flow or from some more complicated mechanism depending on the internal structure of the material (Kauzmann, 1941).

The development of the rate equation as expressed in equation (2-10) is based on a single molecular mechanism. However, this need not be true since in a given material different mechanisms may be operating simultaneously, each having its own characteristic values of ΔH , ΔS , V_f , λ , and λ_l (Kauzmann, 1941).

$$\dot{\gamma} = \sum_{i} \frac{2\lambda_{i}}{\lambda_{l_{i}}} \frac{kT}{h} e^{-\Delta H_{i}/RT} e^{\Delta S_{i}/R} \sinh \frac{V_{f_{i}}}{2kT} \tau \qquad (2-13)$$

where the sum is over all possible mechanisms. Usually, only one of

the mechanisms (i.e., only one of the terms in equation (2-13))will account for the greater part of the observed rate, but it is possible that a single term will not give a major part of the shear rate under all conditions of stress and temperature. For example, one mechanism may account for most of the creep under low stresses, while under large stresses a different mechanism may be dominating. Each mechanism contributes something to the total observed rate under all conditions.

Allied to this generalization of the simultaneous operation of many different mechanisms is the question of the interpretation of strain-hardening in terms of the present theory. This phenomenon is the result of the dependence of the constants in equation (2-13) on time and strain. Thus, hardening could result from an increase in ΔH or from a decrease in ΔS and V_f (Kauzmann, 1941).

Application of Rate Process Theory to Creep of Frozen Soils

One of the major difficulties encountered in the application of the theory entails the measurement of the true value of the shearing stress \mathcal{T} , which acts on the flow unit. The value of the shearing stress \mathcal{T} may vary greatly from one flow unit to another depending on applied stress conditions and structural aspects of the frozen mass. It is important to note that the frozen mass is a skeletal framework of soil particles and ice or aggregated particles and ice crystals, and

not a continuum, so that the shearing process is not a single glide of perfect lattice planes.

Since the appropriate values of \mathcal{T} and $\hat{\mathcal{T}}$ cannot be determined, the following two assumptions are made:

- 1. The rate process theory, equation (2-10) applies to the mean values of the microscopic shear stress $\mathcal T$, and the microscopic shear rate $\mathring{\mathcal T}$.
- 2. These mean values of \mathcal{T} and $\mathring{\mathcal{T}}$ are proportional, respectively, to the macroscopic octahedral shear stress (\mathcal{T}_{oct}) and octahedral shear rate of deformation ($\mathring{\mathcal{T}}_{\text{oct}}$).

For triaxial loading, the principal stress difference ($\mathcal{O}_{I} - \mathcal{O}_{III}$) and the major principal strain \mathcal{E}_{I} , are conveniently measured. Under constant volume conditions with $\mathcal{O}_{II} = \mathcal{O}_{III}$ and $\mathcal{E}_{II} = \mathcal{E}_{III}$, the octahedral shear stress is given by $\mathcal{O}_{oct} = \frac{\sqrt{2}}{3} (\mathcal{O}_{I} - \mathcal{O}_{III})$ and the octahedral shear rate of deformation is $\mathcal{O}_{oct} = \sqrt{2} \, \dot{\mathcal{E}}_{I}$. \mathcal{O}_{III}) is called the deviator stress in the nomenclature of

For uniaxial loading $\tau_{\rm oct} = \frac{\sqrt{2}}{3} \sigma$ and $\dot{\gamma}_{\rm oct} = \sqrt{2} \dot{\epsilon}$. σ and $\dot{\epsilon}$ denote the applied axial stress and the axial rate of deformation respectively.

soil mechanics.

Equation (2-10) can now be rewritten in terms of the measurable quantities σ and ϵ as follows:

$$\dot{\epsilon} = \sqrt{2} \frac{\lambda}{\lambda_1} \frac{kT}{h} e^{\Delta S/R} e^{-\Delta H/RT} \sinh \frac{\sqrt{2}}{3} \frac{V_f}{2kT}$$
 (2-14)

For experimental purposes and at a constant temperature, equation (2-14) has been used as follows: (Dorn, 1954)

$$\dot{\epsilon} = K \sinh BC$$
 (2-15)

Where
$$K = \sqrt{2} \frac{\lambda}{\lambda_1} \cdot \frac{kT}{h} e^{\Delta S/R} e^{-\Delta H/RT}$$

and $B = \frac{\sqrt{2}}{3} \cdot \frac{V_f}{2kT}$

or a more detailed version with temperature effects of the form

$$\dot{\epsilon} = S e^{-\Delta F/RT} \sinh BC$$
 (2-16)

where S is a structure term, sensitive to stress history, temperature history, the instantaneous values of stress and strain.

To obtain a detailed creep equation for frozen soils, in light of the previously developed rate equation, one must evaluate the proper terms (S, Δ H, Δ F, B, etc.) and determine their functional dependence on the external variables, namely, the applied stress and temperature.

In order to study the effect of the external variables on the rate of deformation, one must separate their effect on the structure from their effect on the controlling mechanism. Thus, the influence of stress and temperature should be examined at conditions of constant structure. Conditions of constant structure do not prevail throughout the process of creep. It is precisely these changes in the

structure that cause changes in the creep rate under constant conditions of stress and temperature. Most structural changes during creep of frozen soils take place during primary creep, as indicated by the rapidly decelerating creep rate over primary stage. These changes take place in a relatively short time. After the secondary stage (undamped creep) is reached the change in creep rate is comparatively small, reflecting the smaller change in structure.

The rate process theory applies only to steady state flow.

This restricts its application on frozen soils to secondary creep in the undamped region or to regions in the damped creep where constant rate of creep can be assumed over short intervals.

If equation (2-16) expresses steady state flow under constant stress, then S, ΔF and B should be constants, while in transient creep one or more of these terms are changing. Transient creep implies that molecular processes responsible for macroscopic deformations are not occurring at a constant rate. Therefore the application of the rate theory successfully in the transient region is very doubtful.

In order to isolate the effect of stress on the creep rate, the stress reduction method was employed to provide necessary creep data relating deformation mechanisms to applied stress, independent of structure. In this type of test changes in stress are made during the test. If changes are small and rapid enough, the structure should

remain constant and the effect measured will be related to the deformation mechanism. The details of this technique and other experimental methods are discussed in the next chapter.

CHAPTER III

EXPERIMENTAL TECHNIQUES

To examine the influence of stress on the creep rate, several techniques may be employed providing a wide spectrum of data. In order to evaluate the possible advantages and disadvantages of each method, an outline of these techniques is presented here.

Stress Reduction Method

This method has been used extensively by Dorn (1954) in isolating the effect of stress alone on the creep rate of polycrystalline aluminum.

The method is simple. A frozen soil specimen is precrept at a given deviator stress $\mathcal{O} = (\mathcal{O}_{I} - \mathcal{O}_{III})$ and temperature to a selected conventional strain (change in length of specimen divided by the initial length), at which time the stress is reduced to some lower value of the deviator stress. The instantaneous true creep rate $\dot{\epsilon}_2$ (with $\dot{\epsilon}$, the true strain, namely, the natural logarithm of the instantaneous length to the initial specimen's length) following reduction of the deviator stress \mathcal{O} by $\Delta \mathcal{O}_1$ will then be determined. Second, third, etc., the method is applied to duplicate samples under identical conditions except that the deviator stress is reduced by larger values, $\Delta \mathcal{O}_2$, $\Delta \mathcal{O}_3$, yielding

yet lower instantaneous creep rates, $\dot{\mathfrak{E}}_3$ and $\dot{\mathfrak{E}}_4$. Inasmuch as precreep conditions are identical in each series of tests, the instantaneous structures obtained immediately following an abrupt decrease in deviator stress must necessarily closely coincide with those that prevailed just before the deviator stress was reduced. This will indicate that the change in instantaneous creep rate $\Delta \dot{\mathfrak{E}}$ is due to the change in deviator stress $\Delta \mathcal{C}$ alone excluding any influence of a structure factor on the change in instantaneous creep rate. This method is illustrated in Figure 5-1.

Successive Stress Reductions Method

This method is basically the same as the stress reduction method except that each specimen is subjected to several reductions in deviator stress.

At a predetermined conventional strain, the precreep stress is reduced to a lower value of the deviator stress followed by a second reduction, a third reduction, etc. The number of reduction steps, the amount of each reduction, and the time interval between successive reductions depend on the precreep stress and test temperature. This method is illustrated in Figure 5-3.

Varying Stress-Constant Strain Method

Duplicate specimens are crept under different deviator stress values, ranging from C_1 to lower values of C_2 , C_3 , etc. where $C_1 leq C_2 leq C_3 leq C_4$.

For a selected conventional strain, the corresponding instantaneous creep rates are $\dot{\epsilon}_1 > \dot{\epsilon}_2 > \dot{\epsilon}_3 > \dot{\epsilon}_4$. The instantaneous creep rate in this type of test reflects not only the effect of applied stress, but also the effect of stress history on the substructure of the frozen sample since each specimen is subjected to a different creep stress from the start.

If the variation in applied deviator stress is relatively small, identical structures may be approximated at a selected strain for a particular series of tests. This is illustrated schematically in Figure 3-1.

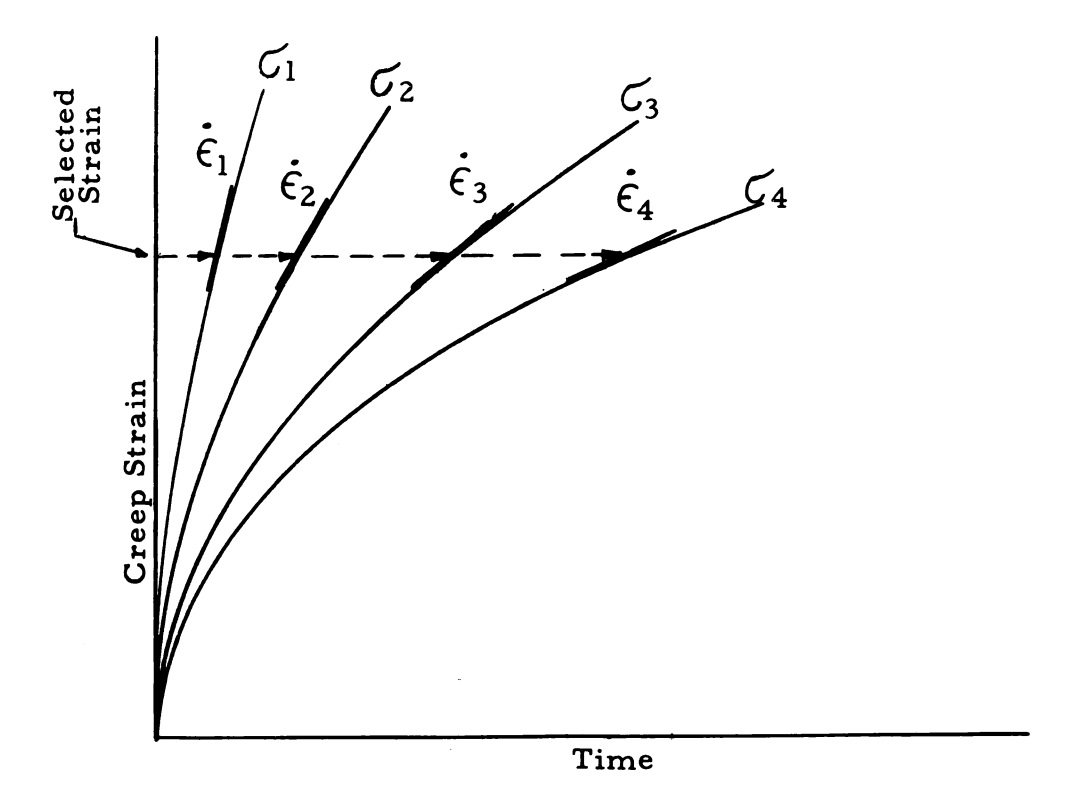


Figure 3-1. Varying Stress-Constant Strain Method

Varying Stress-Constant Time Method

This method is similar to the previous one except that instantaneous creep rates are determined at a selected time instead of a selected strain. This is illustrated schematically in Figure 3-2.

The objection here is that comparing test specimens on the basis of constant elapsed time since the start of the test also means a different structure for each specimen.

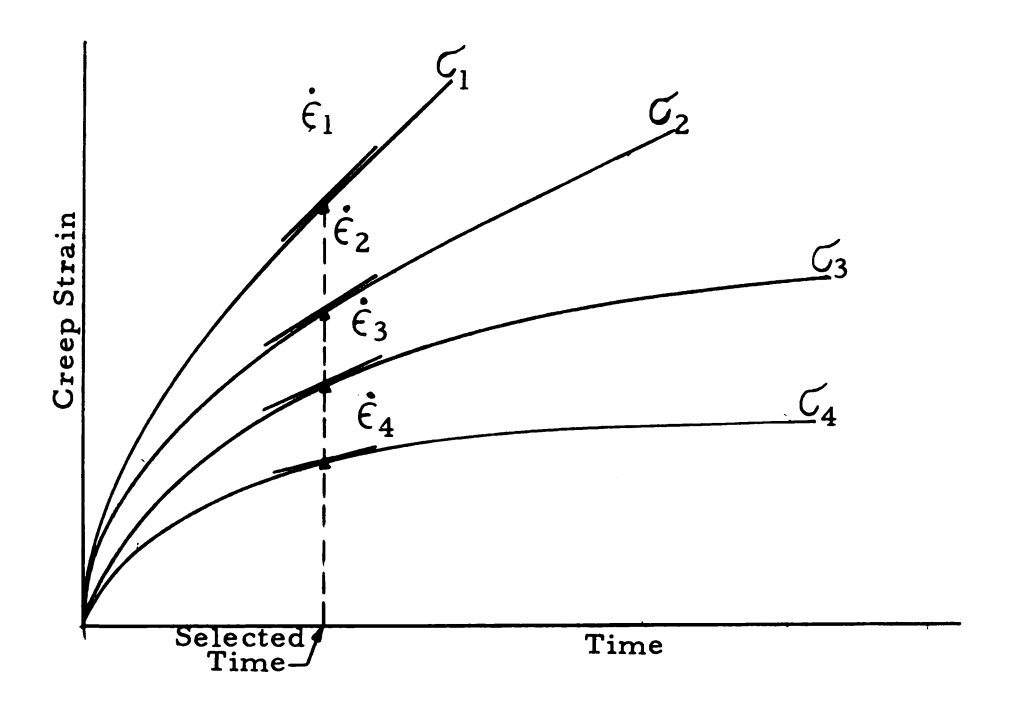


Figure 3-2. Varying Stress-Constant Time Method

Comparison of Various Techniques

In attempting to isolate the effect of deviator stress on creep rate of frozen soil specimens under constant temperature, the structure factor should remain constant throughout a series of tests in order to obtain meaningful results. This may not be secured if the constant

time or constant strain methods are used, since a different stress history may lead to variations in the substructure.

It appears that the single stress reduction method would secure an identical structure and consequently givereliable data. However, the major objection to this method is the fact that each point for the deviator stress-creep rate relationship is obtained from a new specimen and some sample variations are expected. The single and successive stress reduction methods have been used extensively in this study in order to minimize structural differences. The constant strain and constant time with varying stress methods were also attempted for comparison purposes. Upon applying the stress reduction methods, it was found that several factors should be considered for proper analysis of the data.

- 1. It might be suspected that creep recovery immediately following the reduction in stress would interfere with accurate evaluation of the instantaneous true creep rate.

 However, preliminary data indicated that such recovery was not measurable for specimens crept at high stresses, provided single reduction of the stress or successive reductions do not exceed approximately one-third of the initial stress.
- If the stresses are reduced too much, long times will be required to get accurate creep rates. During such

intervals of time, the structure may change from the instantaneous one generated during precreep treatment. Consequently, the range of stresses available for investigation are limited to those that give measurable instantaneous strain rates.

- 3. Change in volume during loading and subsequent creep could alter sample cross-sectional area. Preliminary measurements showed no measurable volume change for the frozen samples used in this study. Hence, equivoluminal deformation has been assumed.
- 4. The extreme sensitivity of frozen soils to temperature history is known to alter the frozen water content and in turn the strength of the frozen media. Therefore, samples used in each series of tests were subjected to identical temperature history in order to eliminate the influence of history variations on the structure.
- 5. It is known that negative pore pressures may exist in the unfrozen water within the frozen mass. However, recent work by Williams (1963) reveals that such negative pore pressures can only be estimated for temperatures down to about -1°C. The temperature range used in this study

is well below -1 °C. Therefore, negative pore pressures are omitted and the analysis has been based on total stresses.

6. After a number of specimens had been tested with the single stress reduction method, the successive stress reduction method was tried. Although identical structures may not prevail in principle during all reduction steps, test data indicates comparable results to the single reduction tests. Data reveal that if reduction steps are applied for short intervals, no significant change in the stress-creep rate relationship is observed. The main advantage in using the successive stress reduction method is the fact that more data may be obtained per sample.

CHAPTER IV

EXPERIMENTAL PROGRAM

Soil Studied

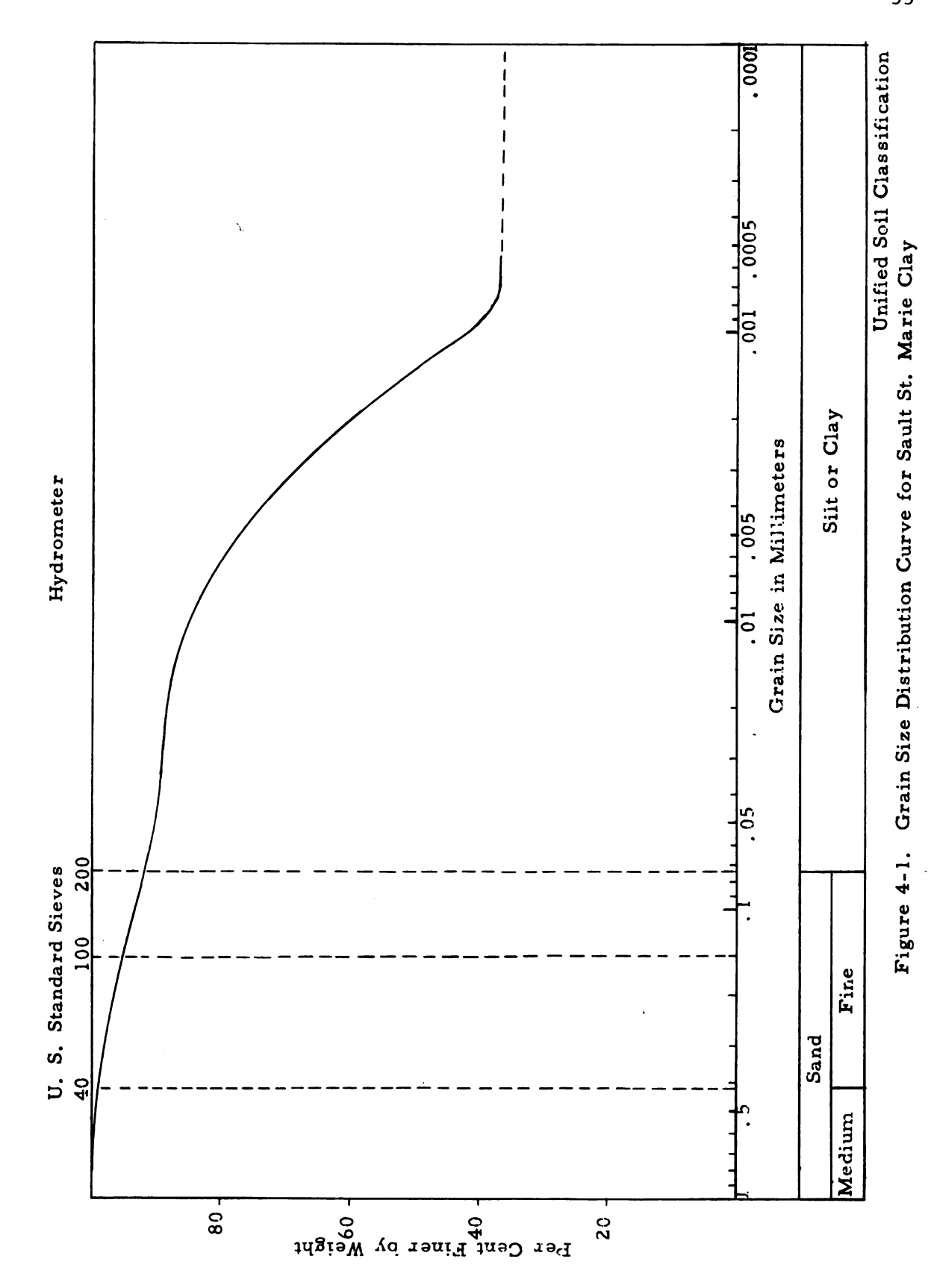
The soil selected for this study is a red clay obtained from a glacial lake deposit approximately 15 miles south of Sault St. Marie, Michigan. It is pedologically classified as Ontonogan. This soil has been used extensively in previous investigations at Michigan State University (Christensen and Wu, 1964; Wu, Loh, and Malvern, 1963).

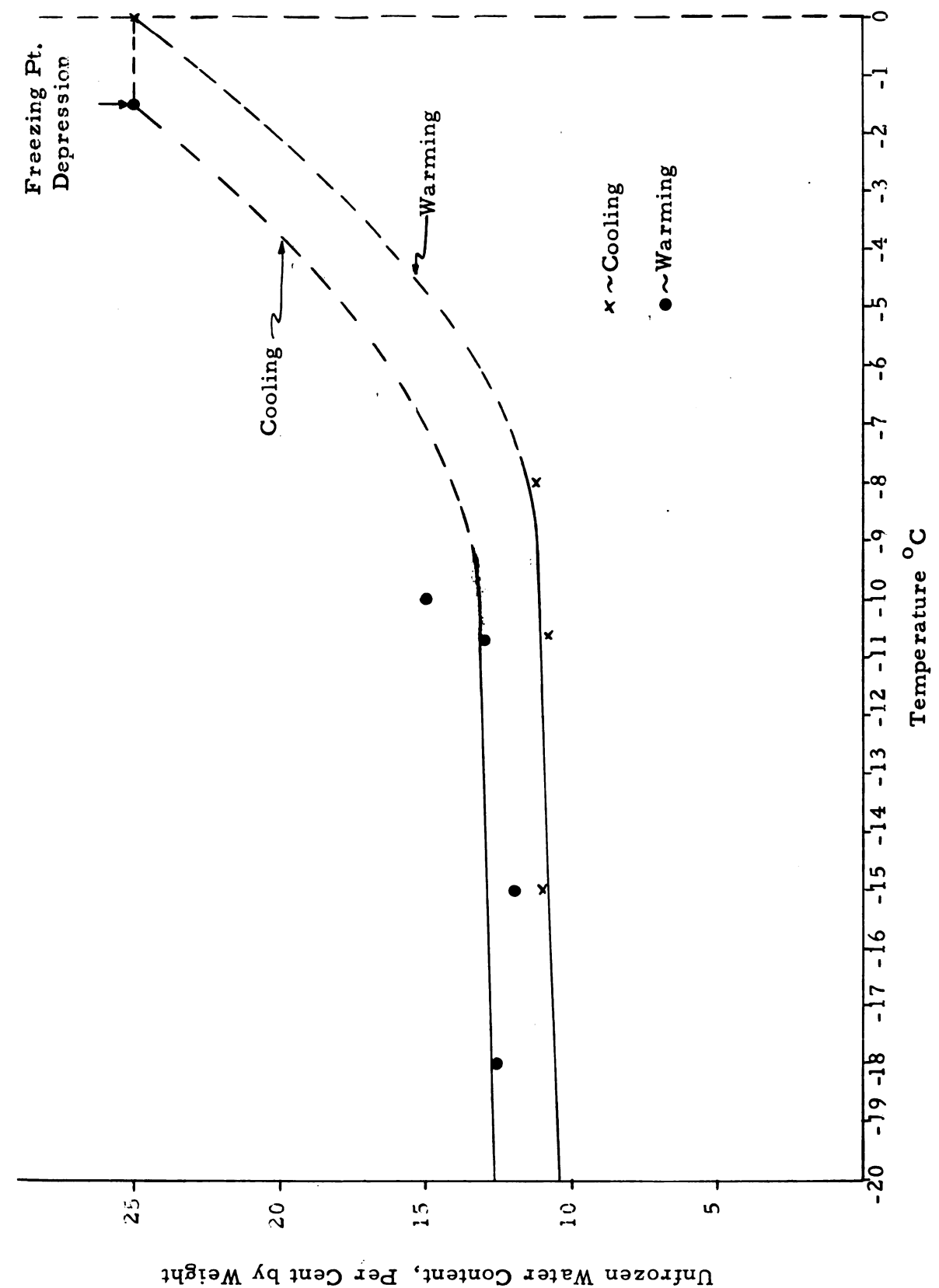
The results of identification and minerological tests on the clay soil are summarized in Table 4-1. The grain size distribution curve (Figure 4-1) shows the relative percentage of sand, silt and clay fractions according to the Unified Soil classification system.

Unfrozen water contents for the temperature range used in this study are shown in Figure 4-2.

TABLE 4-1. Index Properties of Sault St. Marie Clay

Properties	Per Cent or Number
Liquid Limit	60%
Plastic Limit	24%
Plasticity Index	36%
Specific Gravity	2.78
Per cent less than 2 μ	60%
Specific surface area (%∠2 Д)	60% 290-360M ² /gm
Mineral Content (%∠2Д)	
Illite	50%
Vermiculite	25%
Chlorite	15%
Quartz, Feldspar and Montmorillonite	10%





Unfrozen Water Content - Sault St. Marie Clay (After Dillon, in Preparation) Figure 4-2.

Sample Preparation

The red clay was allowed to air dry and was processed by crushing and sieving until all material passed the 1/4 inch sieve; it was then stored in a galvanized can. To minimize initial structural differences among test specimens, duplicate samples were prepared. This was achieved by molding a large cake of soil and cutting it into a number of duplicate samples. Preparation of the 11 inch diameter by 3-1/2 inch high cake involved mixing uniformly predetermined amounts of air dry soil and distilled water. The moistened soil was left to stand for two days in a covered container to ensure an even water-content distribution.

The prepared soil was placed in a compaction ring and compacted statically following the procedure developed by Leonards (1955).

After removal from the ring, the cake was sliced into 21 pieces, each approximately 2 inches square in cross-section and 4 inches in height. The pieces were then wrapped in aluminum foil, waxed and stored in a container under water for at least a week prior to trimming.

Each piece was trimmed to approximately 1.4 inches in diameter and 2.8 inches in height using a motorized soil lathe. Sample measurements included height, diameter, and weight. The initial water content for each sample was checked. Lucite discs were placed on each end of the sample with specially prepared friction

reducers. A layer of silicone grease was spread around the lucite discs. The friction reducers consisted of a perforated sheet of aluminum foil coated with a viscous mixture of silicone lubricant and graphite powder covered with a thin polyethylene sheet on top and bottom. Rubber membranes were placed over the sample with tight fitting rubber bands placed around the lucite discs thereby preventing any leakage during testing or any loss of moisture prior to testing.

The maximum measured variations in water content and in dry density of individual samples within a cake were less than 0.5% and 1 lb/cu ft respectively. Cake design was based on a 100 lb/cu ft unit dry weight and 96% degree of saturation, which meant a water content of 25.5%. The molded water content and the average dry density for the three cakes used in this study are listed in Table 4-2.

TABLE 4-2. Molded Moisture Contents and Average Dry Density of Soil Cakes (Sault St. Marie Clay)

Cake No.	Molded Moisture Content	Average Dry Density
A-1	25.68%	98.04 lb/cu ft
A-2	26.02%	98.08 lb/cu ft
A-3	26.33%	98.09 lb/cu ft.

Test Setup

Trimmed soil samples were mounted in the triaxial cell and secured in place on the pedestal of the cell. Electric tape was wrapped

around the lucite disc and the upper part of the pedestal, thereby preventing any lateral movement of the mounted soil sample with respect to the cell. Prior to securing the top cap over the base, the friction reducers were checked for ease of sliding between the lucite caps and the top and bottom of the sample. If any friction was observed, friction reducers were replaced with new ones.

To freeze the soil sample, the cell was filled quickly with the coolant, a mixture of ethylene glycol and water. Then the cell was centered in the cold temperature tank where the coolant circulates at a set temperature maintained by a low-temperature bath. The sample was cooled at least three degrees centigrade below test temperature, then warmed up to the test temperature after 12 hours and held at the test temperature for an additional 12 hours to insure temperature equilibrium.

Cycling of sample temperature from cooling to warming and back to cooling alters the unit weight and weakens the sample due to expansion of water on freezing. Several samples were subjected to this cycling in temperature at the initial stage of testing due to temporary failure of temperature control of the low-temperature bath. Those samples were considered as preliminary samples and their results are not reported here.

The low-temperature bath was controlled by a mercury thermostat submerged in the bath. The temperature difference

between the tank and the bath did not exceed half a degree centigrade. Periodic adjustment of the thermostat setting was necessary during the summer months because of temperature fluctuation within the room. Temperature measurements were made using copperconstantan thermocouples placed adjacent to sample, in the triaxial cell, and in the tank and connected to a Leeds and Northrup potentiometer, Model K-2. A bath of distilled, deionized, melting ice was used as a reference temperature. A standard cell and Leeds and Northrup Galvanometer aided in temperature measurements. The potentiometer and galvanometer were powered by a standard 6-volt battery. The temperature measuring equipment is shown in Figure 4-3.

Sample temperature did not fluctuate more than \pm 0.05°C after equilibrium was reached. This control was achieved because of the delay in temperature response of the coolant in the triaxial cell. The variation of temperature in the tank was limited to \pm 0.5°C.

Sample Loading and Unloading

After the sample temperature had reached equilibrium, an axial load was applied with an electrically powered mechanical jack.

The initial load corresponding to a selected stress was predetermined, placed on a loading platform and the base of the loading platform was lowered by the jack onto the top of the stainless steel ram in the triaxial cell. The triaxial cell, lucite discs, and several tested

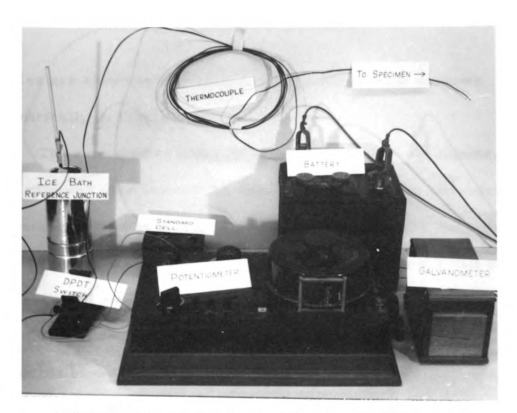


FIGURE 4-3. Temperature Measuring Equipment



FIGURE 4-4. Triaxial Cell and Test Specimens

samples are shown in Figure 4-4. The loading setup is shown schematically in Figure 4-5.

The rate used to lower the load was 1.0 inch per minute. The same rate was used throughout this experimental study to minimize differences in loading history. Friction problems were encountered at the early stage of this study when an aluminum triaxial cell with stainless steel ram was used. The friction was caused by different coefficients of contraction of the metals. The results were corrected afterwards by determining the amount of friction at various temperatures and various stress levels and subtracting the estimated friction for each incorrect test from the initial applied stress. This friction problem affected only several samples in Cake A-1. Afterwards, an all-steel triaxial cell was used, thus minimizing any friction between the ram and the bushing due to the cold temperature. The stainless steel ram was kept lubricated with light oil to eliminate any possible friction in the ram. Normally, the ram falls slowly under its own weight prior to the application of the load.

Upon sample deformation the constant compressive stress was maintained by adding dead weights to compensate for the small increase in sample cross-sectional area. A Syntron Vibro-Flow Feeder permitted uniform addition of lead shot at readily selected rates corresponding to the strain rate of the sample. Part of the initial dead load consisted of preselected amounts of lead shot in buckets

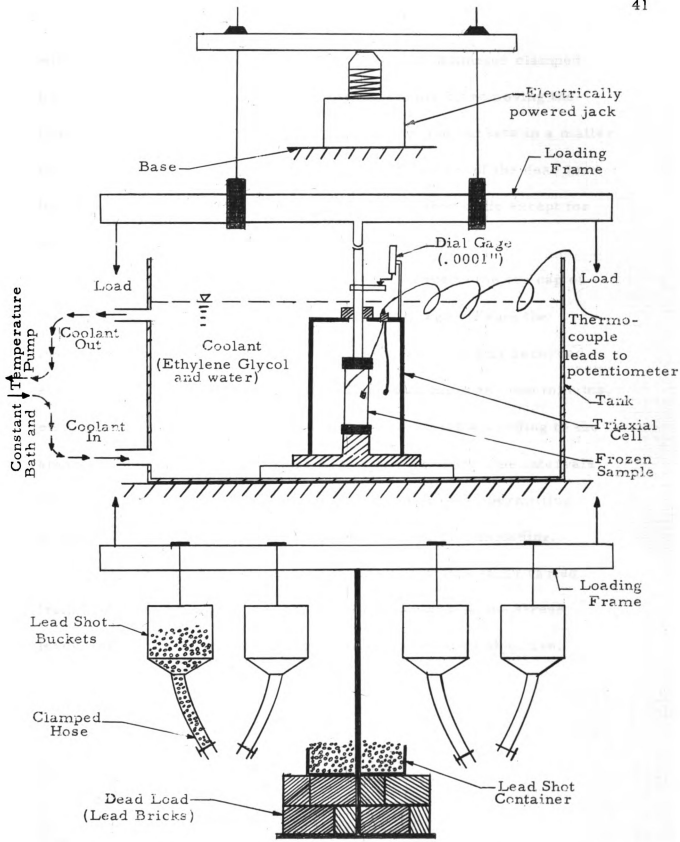


Figure 4-5. Schematic Diagram of the Constant Temperature Stress Reduction Semp

with funnel shaped bottoms connected to a 1 inch diameter clamped hose. Stress reduction was accomplished simply by removing the hose clamps permitting lead shot to drain from the buckets in a matter of seconds, or by carefully lifting an accessible part of the dead load by hand. No confining pressure was applied in this study except for about a 6 inch head of cooling liquid on all samples.

Sample deformation was measured relative to the top cap of the cell, using a 0.000l inch per division dial gage. From the instant the creep load was applied, axial deformation was recorded at thirty seconds, one minute, one and one-half minutes, two minutes, etc. The time interval between readings was varied according to the amount of deformation. Readings were taken in short time intervals prior to stress reduction and immediately afterwards, permitting accurate determination of the creep rate upon partial unloading.

The length of the creep tests conducted in this study varied from about one hour to more than a week depending on the stress level, the stress history of the specimen, and the test objective.

CHAPTER V

EXPERIMENTAL RESULTS

Single Stress Reduction

Two typical examples of the single stress reduction technique are shown in Figure 5-1. Each specimen was precrept under constant stress to a conventional strain of 11 per cent at an axial stress equal to 675 psi. This stress was reduced to 625 psi and 600 psi, respectively, and the instantaneous true creep rates before and after stress reductions were determined as shown in Figure 5-1. Although difficulties were anticipated in determining the instantaneous creep rates after reducing the stress, all of the creep curves using stress reduction exhibited good straight lines immediately following reduction of the stress. A summary of creep data obtained for -12°C using this technique is given in Table 5-1 with basic creep data given in Table I and II of the Appendix.

Creep test results have been divided into several series, as shown in Table 5-1, depending on the creep stress and strain. These results are shown in Figure 5-2, where axial stress is plotted against logarithm of the instantaneous creep rate for each sample.

The dependence of the true instantaneous creep rate on the true instantaneous stress for the structure developed in each series of tests is expressed by an equation of the form

$$\dot{\epsilon} = k * e^{BO}$$
 (5-1)

where k^* is a constant and $\frac{2.303}{B}$ is the slope of the line for each test. Equation (5-1) is equivalent to equation (2-15) for the high stress range to which this study was limited. Equation (2-15) may be written as follows:

Series (1), (2) and (3) shown in Figure 5-2 were conducted at 11 per cent conventional strain in the secondary creep region, while series (4) and (5) were conducted at 9 per cent conventional strain which corresponds to the beginning of secondary creep. Series (6) and (7) were conducted in the primary region of creep at 6 per cent conventional strain.

In order to answer some questions regarding the effect of structural changes on the parameters B and K, as expressed in equation (5-2), the following observations are made from Figure 5-2 and Table 5-1.

1. Series (1), (2), and (3), conducted at a conventional strain of 11 per cent and varying precreep stress, indicate that B is almost independent of the precreep stress in the range from 525 to 675 psi, while the K term decreases very slightly with smaller initial stresses. This does not mean

- that B would remain constant for precreep stresses under 525 psi. This is discussed later in the chapter.
- 2. Series (1), (5) and (6) conducted at a stress of 675 psi and varying precreep strains (6 per cent, 9 per cent, 11 per cent) show that the B term is the same for the 9 and 11 per cent strain and is less for the 6 per cent strain. This indicates that the slope of the stress versus logarithm of strain rate relationship decreases with increasing precreep strain until the precreep strain reaches secondary creep where the slope remains almost constant. Little change during secondary creep is indicative of little change in structure. The K term is found to be more structure-sensitive, decreasing with increasing precreep strains even during secondary creep.
- 3. In order to ascertain whether low precreep stresses influence B and K, three single reduction tests were conducted at varied precreep stresses and strains (Samples A-3 (1), A-3 (2), A-3 (10)). Data are tabulated in Table 5-1 and plotted in Figure 5-4. These three tests indicate that B and K have changed considerably from their values in the previous range of high precreep stresses. The changes are an increase in B and a decrease in K. Similar and more explicit data in the low stress range obtained using

the successive stress reduction method, confirmed that B increases while K decreases with decreasing precreep stress.

Successive Stress Reductions

A typical example using several stress reductions on a frozen sample of Sault St. Marie Clay is shown in Figure 5-3. The sample was crept under an axial stress of 675 psi to a conventional strain of 9 per cent. Stress reductions of 40 psi, 37 psi, and 36 psi were made at 9 per cent, 11 per cent, and 13 per cent conventional strains, respectively.

Although precreep conditions had changed slightly at each stress reduction, comparable results to the previous technique were obtained.

This method gives more information per sample and minimizes sampling variations because the same sample is used for several stress reductions.

Test results employing this method are summarized in Table 5-2, and basic creep data given in Table III of the Appendix. A plot of axial stress versus logarithm of the instantaneous creep rate for each sample is shown in Figure 5-4. Successive stress reductions tests were conducted at several temperatures ranging from -3°C to -18°C. Table 5-2 and Figure 5-4 show the variation in B and K with decreasing stresses at several temperatures.

The change in B with temperature change reflects possibly the influence of temperature on the structure. The B parameter increases with increasing temperatures.

The following observations are made regarding the results plotted in Figure 5-4:

- stant above a certain stress level (500 psi). Below this stress level B increases with lower stresses, while K decreases. This same behavior occurs at -15°C and -18°C as shown in Figure 5-4. Thus, the change in B and K suggests a logarithm of creep rate versus stress curve that begins as a straight line and changes with decreasing applied stress to a flat curve, such that B equals 2.303 times the reciprocal of the slope and K equals the intercept of the tangent at zero stress. The straight line portion seems to disappear at temperatures warmer than -9°C.
- 2. Since the plot of stress versus logarithm of creep rate does not show clearly the change in the magnitude of the B term, the following equation has been used to compute B:

$$B = \ln \frac{\dot{\epsilon}_1}{\epsilon_2} / \Delta C_1 \qquad (5-3)$$

where $\dot{\xi}_1$ and $\dot{\xi}_2$ are the instantaneous creep rates determined before and after stress reduction and ΔG_1 is the amount of stress decrease. These values are listed in Table 5-1 and 5-2.

3. The dashed lines in Figure 5-4 correspond to the change in creep rate under constant stress. This is observed mainly in the low stress region (damped creep) and is apparently due to strain-hardening.

Regular Creep

These data were obtained concurrently with the data of stress reductions at constant temperature (-12°C) and several stress levels. Figure 5-5 shows the time-strain relationship during the initial stage of creep, while Figure 5-6 shows the same curves over a period of 200 minutes. Time zero begins at no load. Full load is reached between 1-1/2 to 2 minutes.

The Effect of Stress History on the B and K Parameters

The question now arises as to what effect extended changes in stress history might have on the parameters B and K. It has already been determined that B and K change with decreasing creep stress.

Do B and K retain the same values if different stress history is followed?

To answer this question, several samples that had already rendered their primary function were subjected to additional stress changes at different temperatures. Results are shown in Figure 5-7a through 5-7e, where the stress-strain history is presented with the logarithm of creep rate versus axial stress for each sample. Basic creep data is shown in Table III of the Appendix.

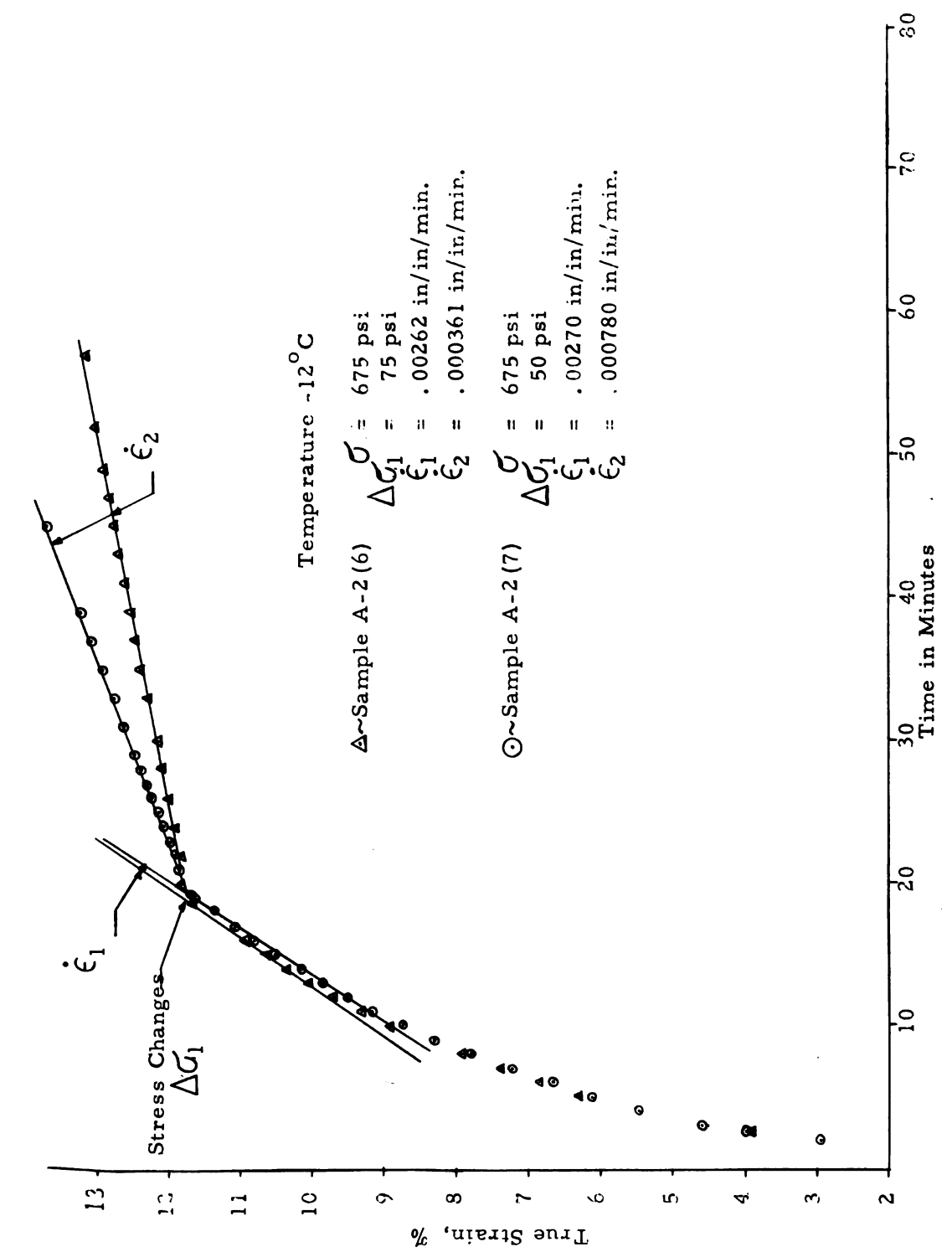
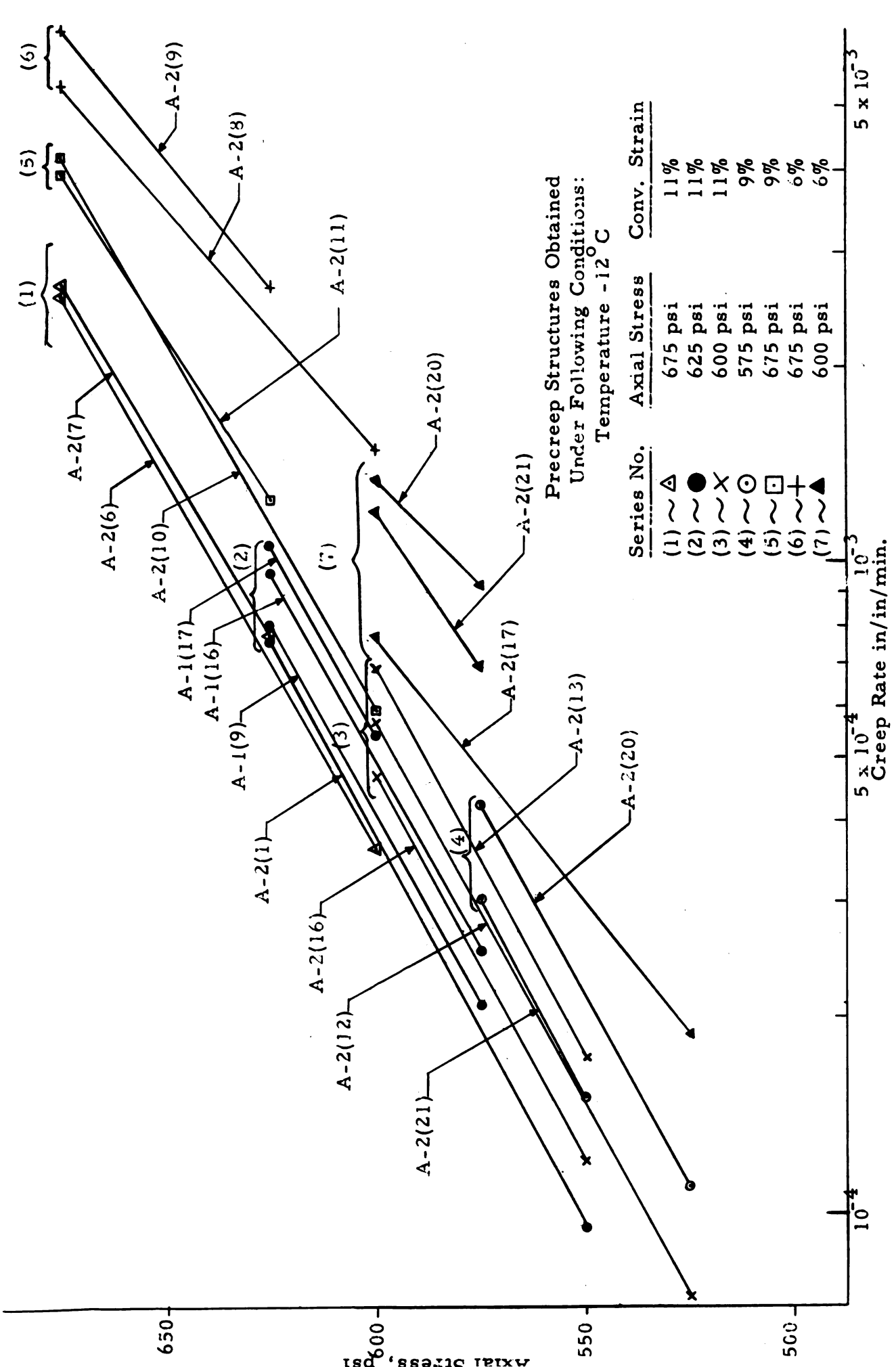


Figure 5-1. Typical Examples of the Effect of Single Stress Reduction on Creep Rate - Sault St. Marie Clay



Effect of True Stress on Greep Rate Using Single Stress Reduction - Sault St. Marie Clay Figure 5-2.

51

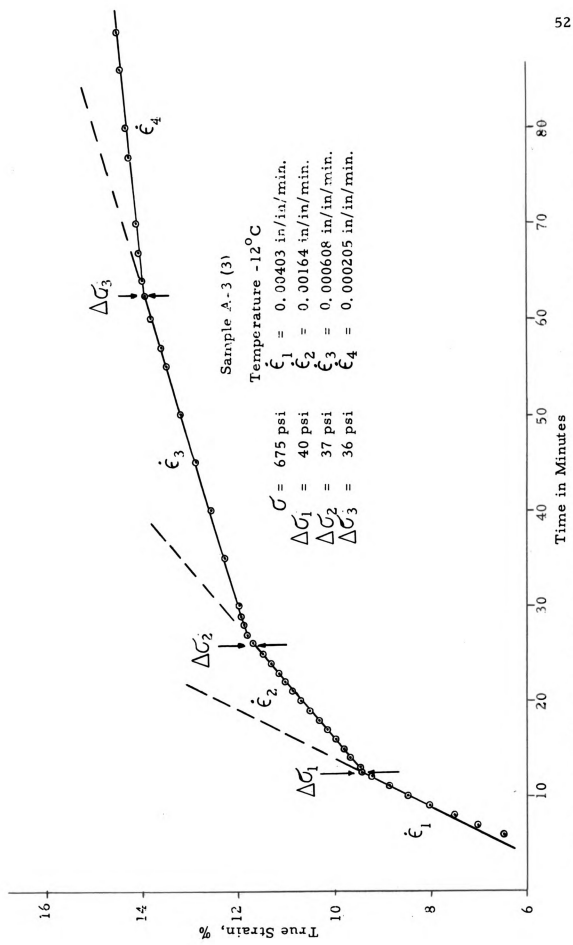


Figure 5-3. Typical Example of the Effect of Successive Stress Reductions on Creep Rate - Sault St. Marie Clay

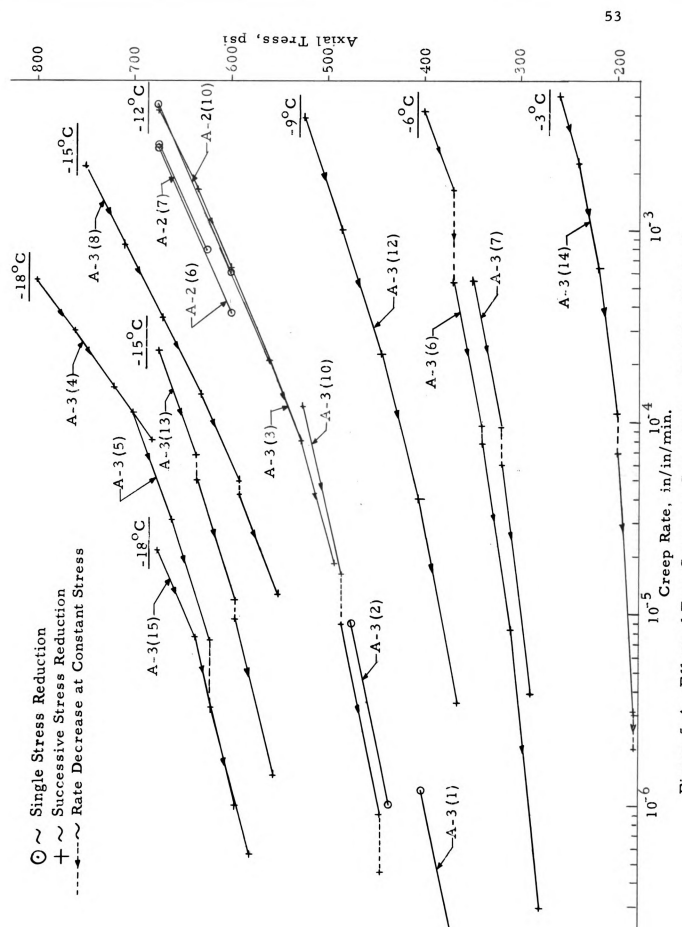
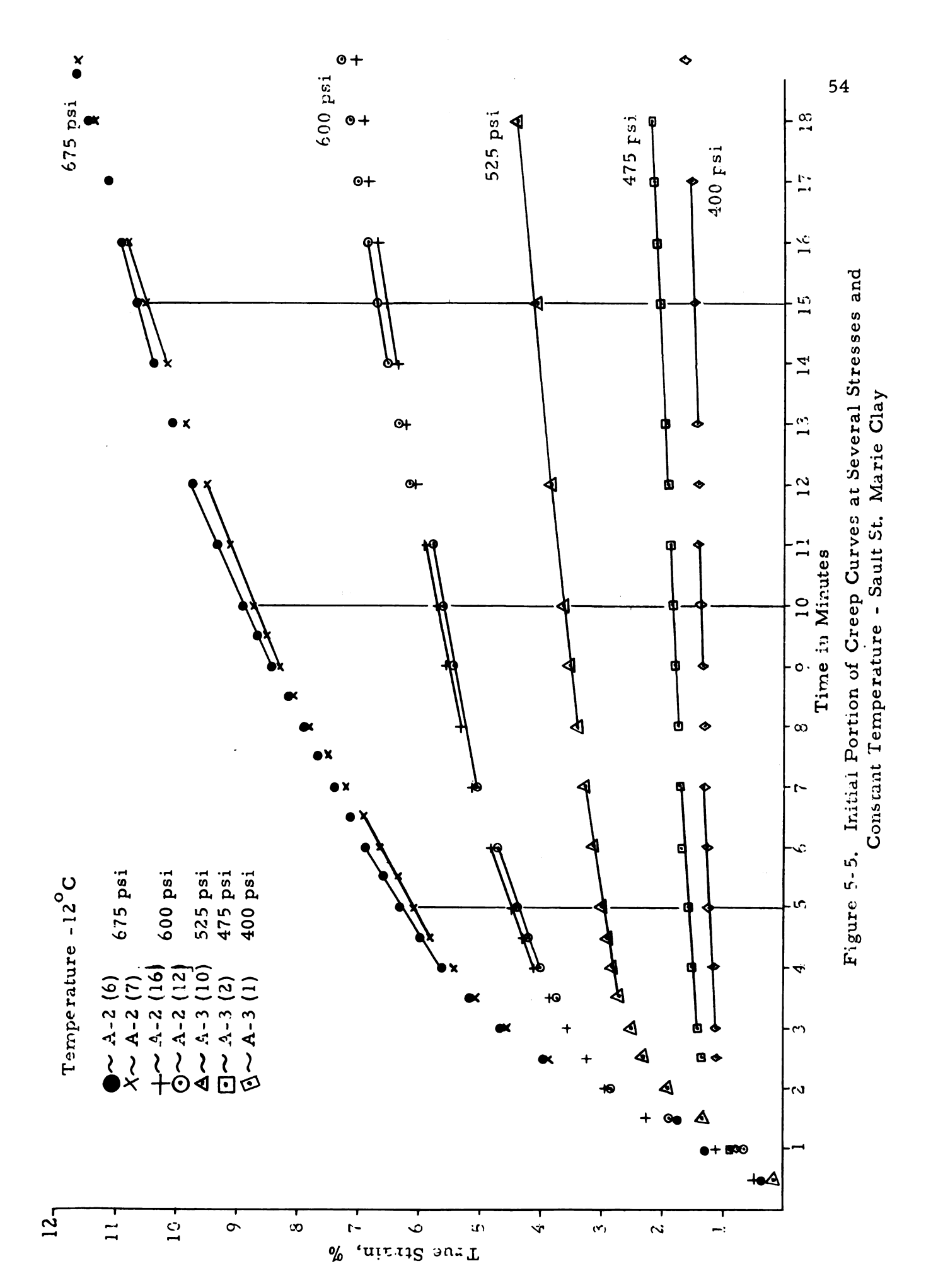
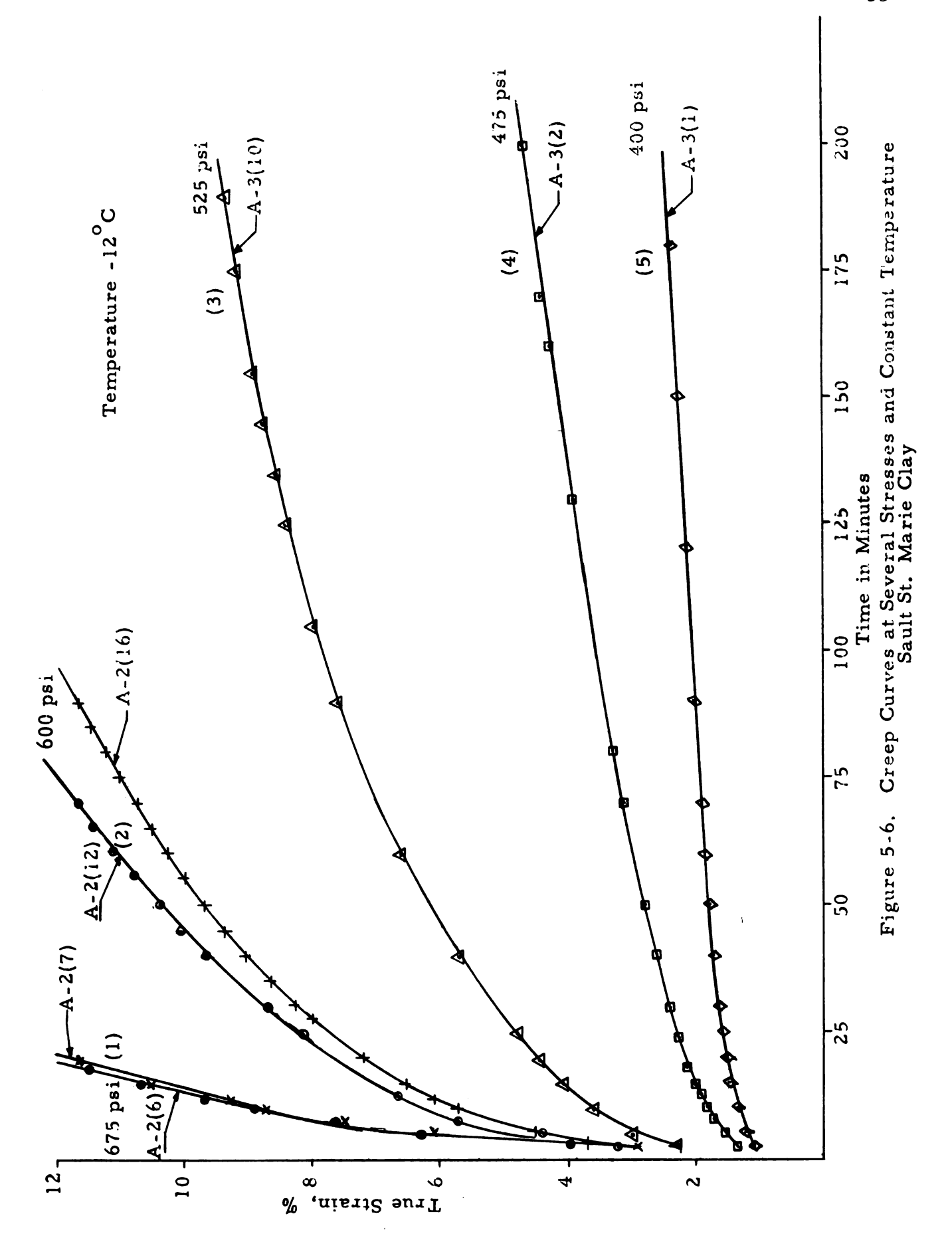
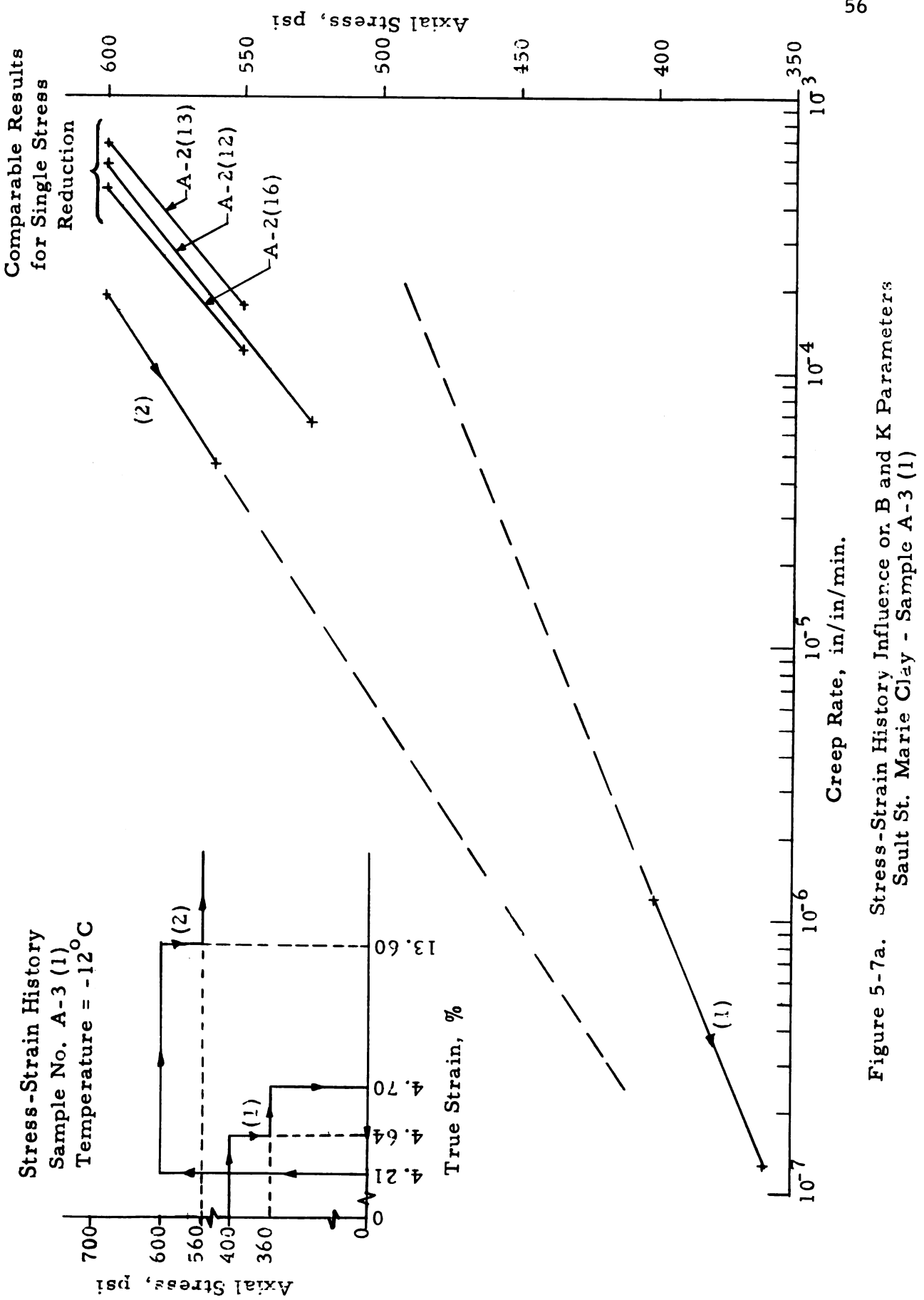


Figure 5-4. Effect of True Stress on Creep Rate - Sault St. Marie Clay









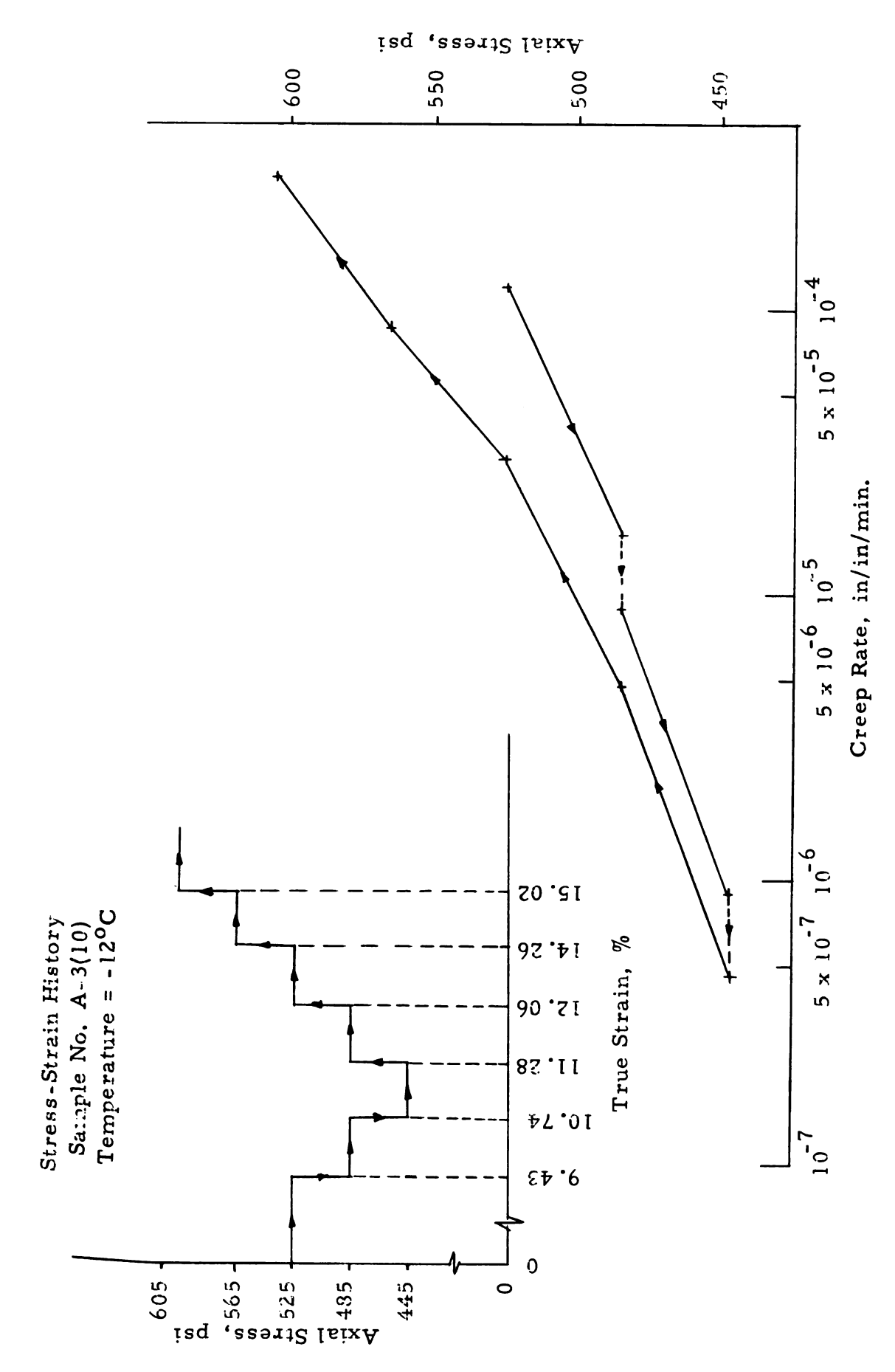
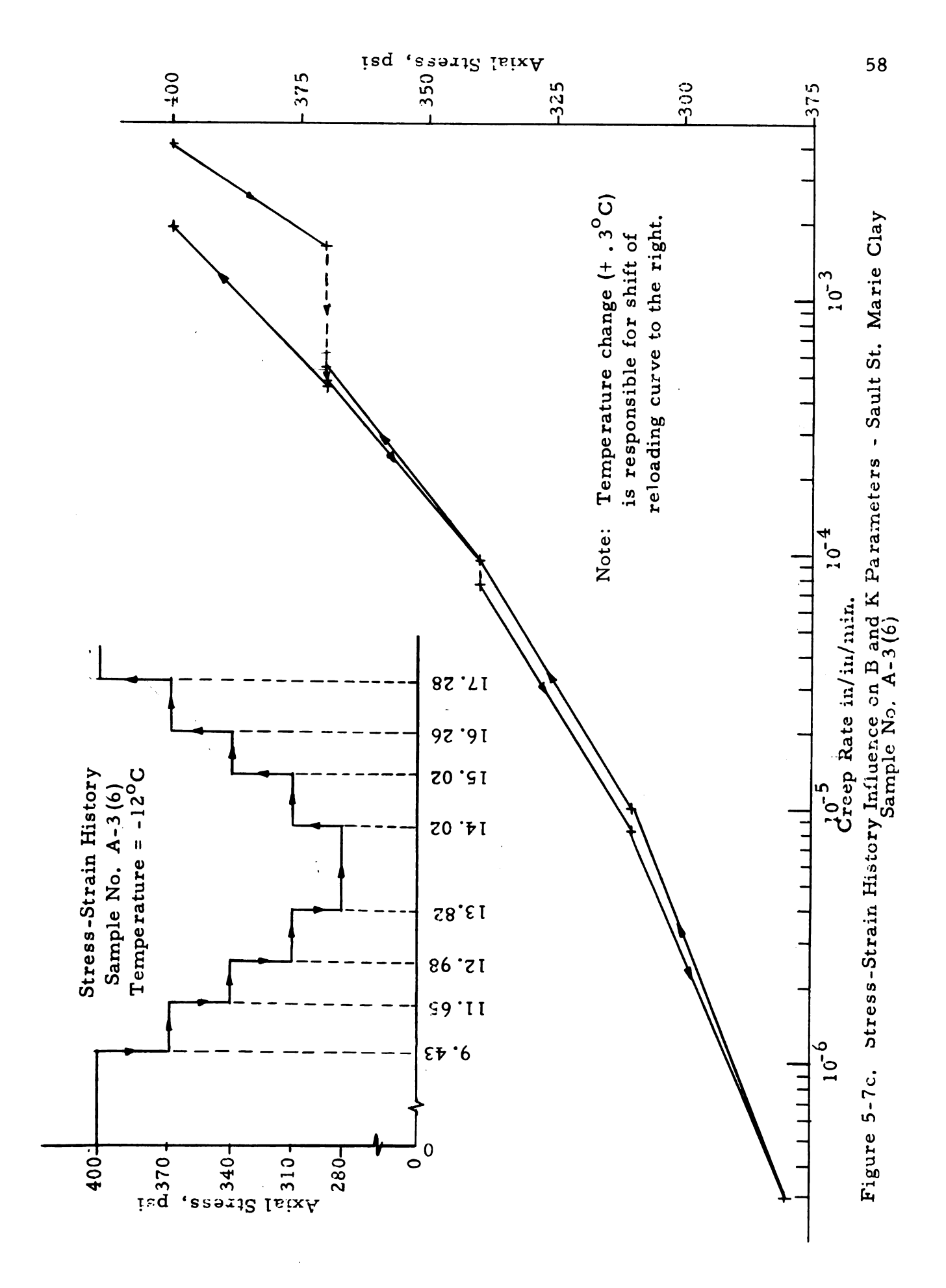


Figure 5-7b. Stress-Strain History Influence On B and K Parameters - Sault St. Marie Clay Sample No. A-3(10)





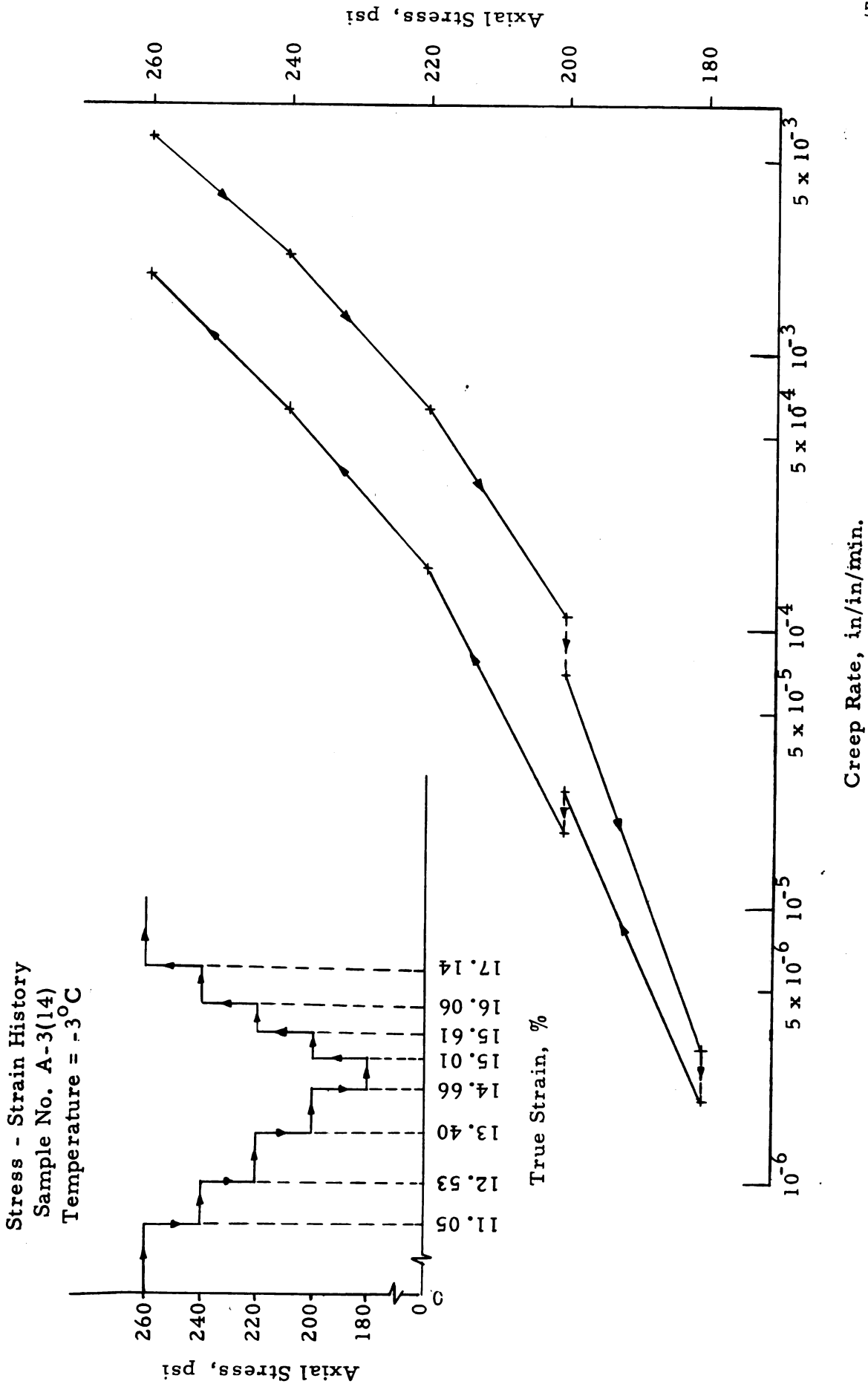
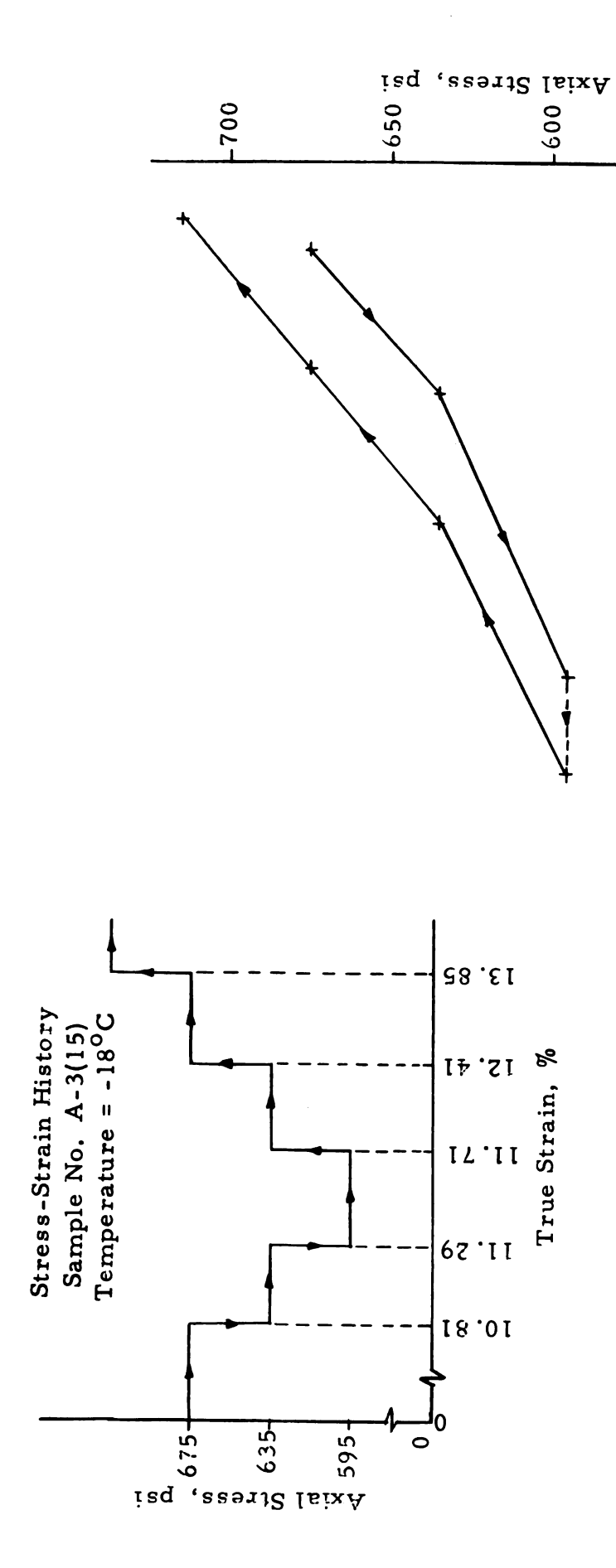


Figure 5-7d. Stress-Strain History Influence On B and K Parameters - Sault St. Marie Clay Sample No. A-3(14)





Creep Rate, in/in/min.

2.758×10⁻² 2.712 " 2.712 " 5.575 x 10⁻² 5.674 " 5.008 " 2.716×10⁻² 2.747 "... 2.632×10² 2.610×10⁻² | 2.307 ".. $\begin{vmatrix} 1.719 \times 10^{-2} \\ 1.856 & ... \end{vmatrix}$ 1.885×10⁻² 1.541 " 2.742×10^{-2} = S (im. /1b.) 2,712 2.099 В 4.5 9.6 Summary of Creep Data on the Sault St. Marie Clay Using Single Stress Reduction (Temperature -12°C) Strain (%) I 11 11 66 9 2 999 1 1 1 1 I Conv. 1.28×10⁻⁷ x 10-5 × 10-2 x 10⁻⁵ 1 x 10⁻⁵ x 10-5 1.62×10^{-5} S S × 10-× 10 . niM = = = = Ξ = = (ini, .ni) г₂ 36.4 78.0 60.0 126.0 150.0 263.0 20.5 25.0 15.0 18.8 92.0 70.0 10.8 54, 5 9.6 425.0×10⁻⁵ 545.0×10⁻⁵ 666.0 " 11.9×10⁻⁷ 90.9 " 12.0×10^{-5} 42.5 \times 10⁵ .niM S S S S 81.5×10⁻⁵ 96.9 " 57.5×10⁻⁵ 68.7 " 77.2×10⁵ 262.0×10⁻⁵ 270.0 " (in. /in.) = = = Ęı 118.0 47.0 76.5 29.6 107.6 (isq) 75 50 50 50 25 75 75 50 50 50 25 75 50 75 50 25 25 25 40 39 40 crease Stress De-(isq) 675 675 625 009 575 675 675 009 475 900 900 sært2 gəəro Initial Pre-25.70 25.70 25.58 25.54 25.40 25,63 25.70 25.55 25.68 25.54 25.40 25.76 25.53 25.46 25.32 25.93 25.72 25, 12 Content (%) Moisture Final 26.02 26.02 25.68 25.68 26.02 26.02 26.02 26.02 26.02 26.02 26.02 26.33 26.33 25,68 26.02 26.02 26.02 26.02 26.02 26.02 Content (%) Moisture Molded 5-1. 98.04 98.04 98.08 98.08 98.04 98.08 98.08 98.08 98.08 98.08 98.08 98.08 98.08 98.08 98.09 98.09 98.09 98.08 98.08 98.08 98.08 (Jp co tt) TABLE Density Molded Dry A-2(10) A-2(11) A-2(17) A-2(20) A-2(12) A-2(13) A-1 (9) A-1(16) A-3 (1) A-3 (2) A-2(21) A - 2(20)A-2 (8) A-2 (9) A-2(21) A-3(10) A-2 (6) A-2 (7) A-1(17) A-2 (1) A-2(16) .oN Sample Series No. (1)(5)(3)(4) (2) 9 (2)

Creep Data on the Sault St. Marie Clay Stress Reductions at Several Temperatures	स (ता \ .ताः)	1.542 x 10 ⁻² 2.742 "	2.099×10 ⁻² 2.712 "	2.251 x 10 ⁻² 2.684 " 3.024 " 2.719 " 4.214 "	5.008 x 10 ⁻² 5.703 "	1.525×10 ⁻² 1.695 " 1.578 "	3.160×10 ⁻² 3.666 " 4.618 "	2.56 × 10 ⁻² 5.037 "
	Conv. Strain (%)	96	9	9 11 13 15 16. 5	9 10. 19	9 11 13	7 8 9.2	10.25 11.68
	÷ (in. /in.) Min.	92.0 ×10 ⁻⁵ 10.8 ''	70.0 ×10 ⁻⁵ 15.0 ''	164.4 × 10 ⁻⁵ 60.8 " 20.5 " 7.9 " 1.82 "	$\frac{1.62 \times 10^{-5}}{9.07 \times 10^{-7}}$	30.0 × 10 ⁻⁵ 15.1 " 8.05 "	3.19×10 ⁻⁵ 7.36×10 ⁻⁶ 5.63×10 ⁻⁷	7.65×10 ⁻⁶ 10.2 ×10 ⁻⁷ 1
of Creep Data on the ive Stress Reductions	(in. /in.) Min.	135.0 × 10 ⁻⁵ 42.5 ''	118.0 × 10 ⁻⁵ 29.6 ''	403.0 × 10 ⁻⁵ 164.4 " 60.8 " 20.5 " 7.9 "	$12.0 \times 10^{-5} \\ 8.88 \times 10^{-6}$	55.2 ×10 ⁻⁵ 30.0 " 15.1 "	11.3 × 10 ⁻⁵ 3.19 " 0.357 "	2.13×10 ⁻⁵ 7.65×10 ⁻⁶
Summary TABLE 5-2. Using Success:	Stress De- crease (psi)	25 50	25 25	40 37 36 35 35	40 40	40 40 40	40 40 40	40
	- Pre-laitial Pre-se Stress (isq)	009	009	675	525	800	700	675
	Final Moisture Content (%)	25, 54	25.40	26.04	25, 12	25.56	26.08	25.89
	Molded Moisture Content (%)	26.02	26.02	26.33	26.33	26.33	26.33	26, 33
	Molded Dry Density (lb/cu ft)	98° 08	98. 08	98.09	98.09	98.09	98.09	98.09
	Sample No.	A-2(20)	A-2(21)	A-3 (3)	A-3(10)	A-3 (4)	A-3 (5)	A-3(15)
	Co.qmeT	-12	-12	-12	-12	-18	- 18	- 18

TABLE 5-2. (Continued)

а (dí\ ^s .ni)	2. 394 × 10 ⁻² 2. 147 " 2. 311 " 2. 61 " 3. 075 "	3.083×10 ⁻² 3.570 " 4.710 "	3.383×10 ⁻² 3.728 " 4.338 " 6.993 "	3.081×10 ⁻² 5.719 " 7.390 "	5.871 × 10 ⁻² 9.163 "	4.972×10 ⁻² 6.29 " 8.70 " 15.64 "
vnoO Strain (%)	9 10 10.5 11	9 9.57 9.76	9 10 10.5 11.0	9 11 12 13	9	11.05 12.54 13.40 14.66
5 (in. /in.) Min.	83.3 × 10 ⁻⁵ 35.3 " 14.0 " 4.93 " 1.28 "	6.82×10^{-5} 1.2 1.44×10^{-6}	100.0 × 10 ⁻⁵ 22.5 " 3.97 " 3.41 × 10 ⁻⁶	163.00×10 ⁻⁵ 9.52 " 8.39×10 ⁻⁶ 2.99×10 ⁻⁷	9.31×10 ⁻⁵ 3.84 "	222.0 × 10 ⁻⁵ 63.2 " 11.1 "6 3.04 × 10 ⁻⁶
F ₁ (in. /in.) Min.	217.0 × 10 ⁻⁵ 83.3 " 35.3 " 14.0 "	23.4 × 10 ⁻⁵ 5.0 " 9.47 × 10 ⁻⁶	386.0 × 10 ⁻⁵ 100.0 '' 22.5 '' 3.97 ''	411.0 × 10 ⁻⁵ 52.9 '' 7.7 '' 8.39 × 10 ⁻⁶	54.2 × 10 ⁻⁵ 6.0 ''	600.0 × 10 ⁻⁵ 222.0 ·!! 63.2 ·!! 6.93 !!
Stress De- cresse (psi)	0 4 4 4 0 4 4 0 0 0 0	04 04 04 04	04 4 04 0 04 0	30 30 30	30	20 20 20 20
-erd IsitinI exext2deero (isq)	750	675	525	400	350	260
Final Moisture Content (%)	25.74	26.16	25.73	25.62	25.37	25.63
Molded Moisture Content (%)	26.33	26.33	26.33	26.33	26.33	26.33
Molded Dry Density (lb/cu ft)	60 *86	98.09	98.09	98.09	98.09	98.09
Sample No.	A-3(18)	A-3(13)	A-3(12)	A-3 (6)	A-3 (7)	A-3(14)
Do .qmaT	15	15	6	9	9	6

CHAPTER VI

DISCUSSION

General

The numerical creep results presented in the preceding chapter show general characteristics typical of a frozen clay soil.

Interpretations that follow include sections on the B parameter and the K parameter.

The unfrozen water content has a significant effect on the stress versus creep rate relationship. This is indicated by the changing shape of stress versus logarithm of creep rate curves at various temperatures as shown in Figure 5-4. The straight line portion of the curve exhibited at low temperatures (-12°C, -15°C and -18°C) and higher stresses disappears at higher temperatures beginning at -9°C. Curves tend to get flatter at warmer temperatures. The plausible explanation to this change in shape is the appreciable increase in unfrozen water content for temperatures warmer than -9°C as indicated in Figure 4-2. This increase in unfrozen water alters the frozen soil structure and in turn changes the bonding strength at the particle contacts. Below -9°C, the amount of unfrozen water changes little with change in temperature (see Figure 4-2); thus, it has a less significant effect on the frozen structure.

At low stresses, strengthening (or strain-hardening)

mechanisms control the creep process, leading to constantly decreasing rates (damped creep) while at high stresses, weakening mechanisms dominate creep, leading to eventual increase in the creep rate and subsequent failure. Damped creep begins when applied stress falls below a limiting stress (critical stress). This is indicated by the definite deviation from the straight line portion in the logarithm of creep rate versus stress relationship shown in Figure 5-4, which corresponds approximately to a creep rate of 10⁻⁴ in/in/min. Although such a deviation is not evident for higher temperatures, the stress corresponding to 10⁻⁴ in/in/min. has been assumed to be the critical stress. A plot of estimated critical stresses, for the temperature range investigated in this work, is shown in Figure 6-4.

It appears that the critical stress is a measure of the limiting long-term strength that frozen soils exhibit under an applied stress. During undamped creep, the strength of the frozen sample is gradually exhausted until it becomes equal to or exceeded by the applied stress. At this point progressive flow begins leading to eventual sample failure. This is shown schematically in Figure 6-1 where (R) denotes the strength of the sample corresponding to a given time since the application of the creep stress. The critical stress ($\mathcal{C}_{\mathbf{C}}$) or its equivalent, the limiting long-term strength, divides creep of frozen soils into two regions, damped and undamped creep. For a given creep stress $\mathcal{C}_{\mathbf{I}}$, time $\mathbf{t}_{\mathbf{I}}$ is required before the resistance of the frozen sample is

completely exhausted permitting progressive flow to take place. For a creep stress C_2 time t_2 is required before the progressive stage begins, etc. If the applied stress falls below the critical stress, sample resistance is greater than applied stress at all times and progressive creep never occurs.

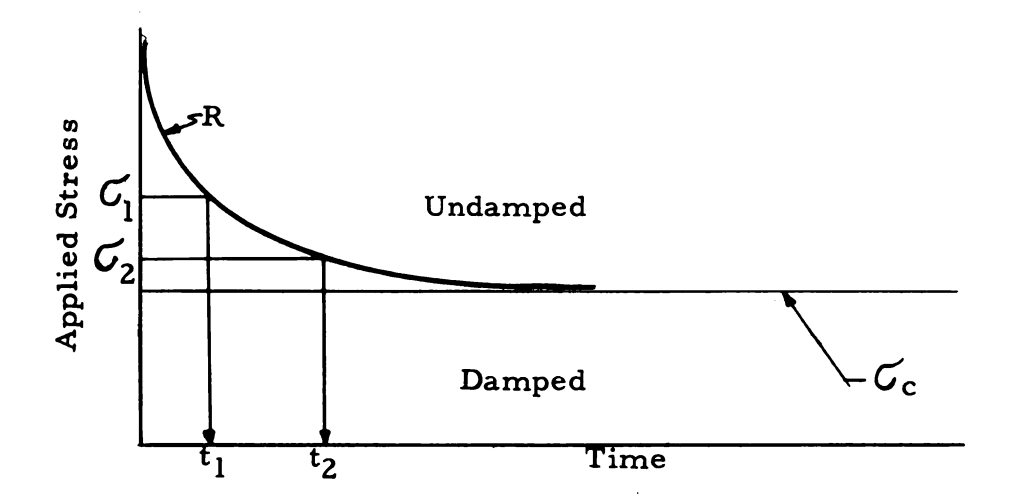


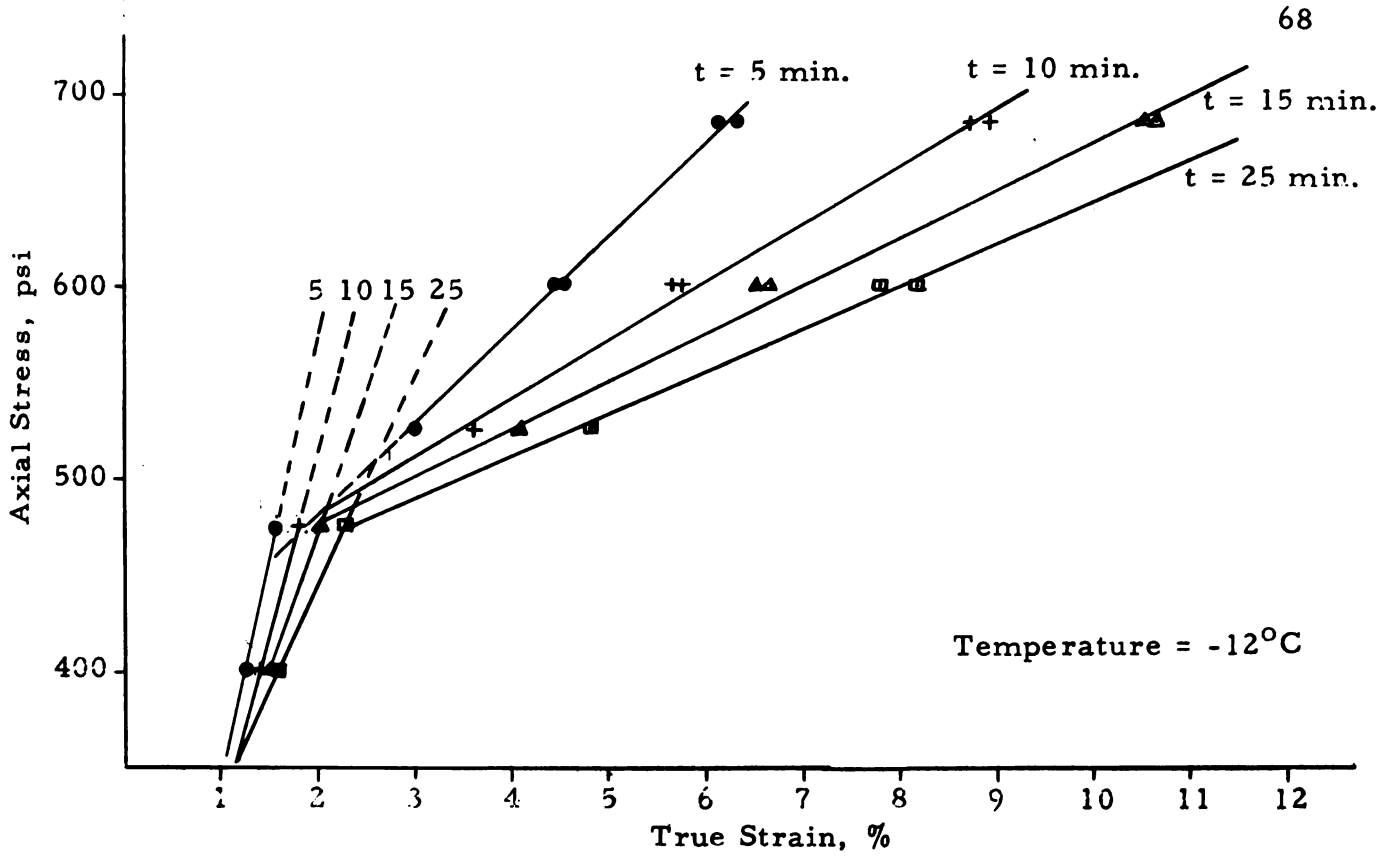
Figure 6-1. Schematic Diagram Showing the Change in Strength of a Frozen Clay Soil with Time

Sample resistance during the creep process is the net result of the strengthening and weakening mechanisms that proceed simultaneously. The strength of the frozen structure is attributed to the bonds between contacts. Such contacts may be particle to particle, particle to ice, or ice to ice contact. Upon application of a stress, these bonds get weaker causing partial or total break-up of bonds. This may be accompanied by pressure melting and refreezing of ice grains within the soil pores. New bonds may form if creep proceeds at a slow rate. The shearing strength at the contact may vary widely

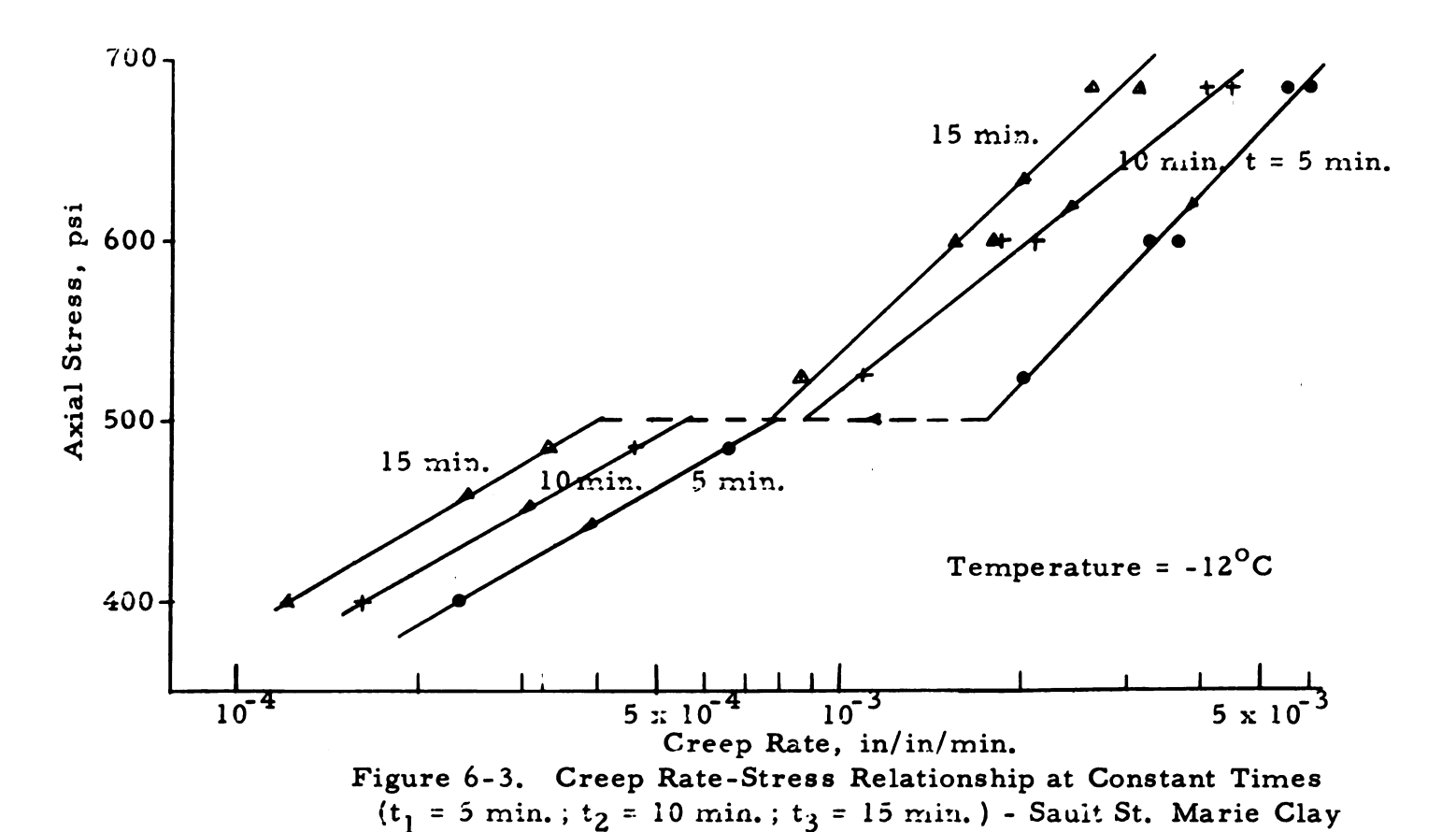
from contact to contact. Such variation would depend on the area of contact and the orientation of the contact surface with respect to the direction of applied stress.

The significance of the critical stress and its effect on creep strain and creep rate is observed by comparing the various creep curves in Figure 5-5 and 5-6. At selected times the values of the true strains associated with curves (1) and (2) are much larger than those of (4) and (5). Stress-strain curves derived from these creep curves are plotted in Figure 6-2 using times (t = 5 min., 10 min., etc.) A definite break in the stress-strain curves is observed between the two stages of creep, damped and undamped. Tests (4) and (5) fall below the so-called critical stress for this temperature, while (1) and (2) are above the critical stress. Critical stress for the -12°C temperature is estimated to be in the neighborhood of 500 psi. A plot of the stress versus logarithm of creep rates at various time intervals, as shown in Figure 6-3, indicates a possible straight line relationship among creep rates (1), (2) and (3) and another line with lesser slope for (4) and (5). An appreciable change in the creep rate between the two straight lines is observed around 500 psi.

The ultimate strength, shown in Figure 6-4, was determined at several temperatures from samples subjected to stresses high enough so that frozen samples did not support the load long enough for actual strain measurements. Failure took place shortly after load



Stress-Strain Curves Derived from Creep Tests Figure 6-2. for Selected Times - Sault St. Marie Clay



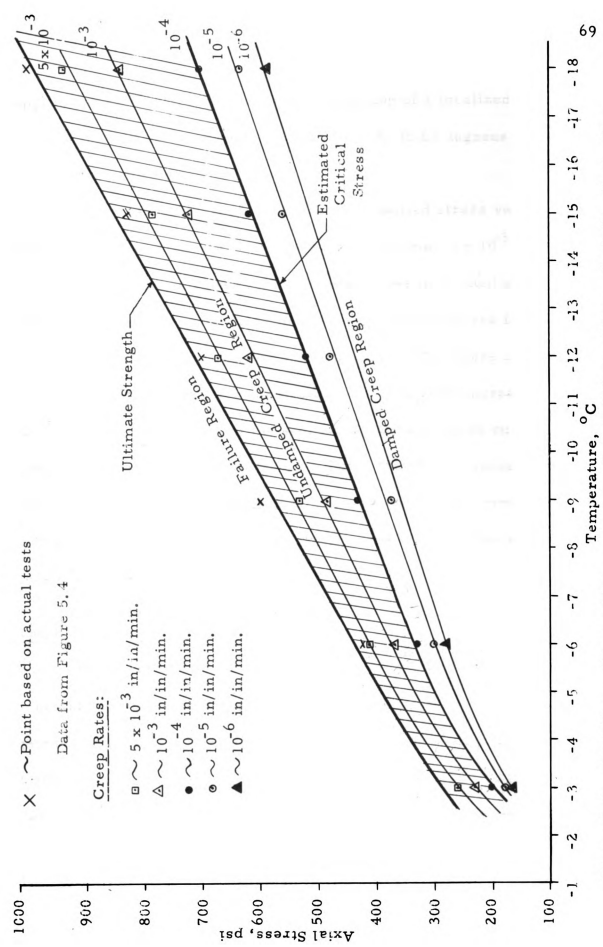


Figure 6-4. Axial Stress Versus Temperature for Selected Greep Rates - Sault St. Marie Clay

application (3-5 min.) and during the formation of a localized failure surface making an acute angle ranging from 45 to 60 degrees with the base of the sample.

Using data presented in Figure 5-4, applied stress versus temperature was plotted at creep rates ranging from 5 x 10³ in/in/min. to 10⁶ in/in/min. as shown in Figure 6-4. This permitted a straight-line plot except for slight curvature at higher temperatures for each creep rate. The curved portion starts around -9°C, where appreciable changes in unfrozen water content begin to occur with increasing temperature. The slopes of the straight portions of these curves decrease with decreasing creep rates. Thus, Figure 6-4 presents a complete picture of data obtained by the stress reduction method permitting a reasonable estimation of creep rates as a function of temperature and axial stress.

The B Parameter

Data presented in Chapter V show that the B parameter is not constant over the entire range of stresses and temperatures investigated in this study. The parameter B appears reasonably constant for a given temperature at stresses that fall in the undamped region.

Below the critical stress B increases with decreasing applied stress as shown by the changing slope in Figure 5-4. The computed variation in B at a constant temperature is listed in Tables 5-1 and 5-2.

The variation is of the order of 200 to 300%.

The increase in the B parameter due to stress decrements could be attributed to the change in the mechanism of deformation, as the creep process shifts from a steady-state type mechanism to possibly different mechanism (or mechanisms) in the damped region of creep. This is accounted for in the rate process theory which assumes a constant B at a constant temperature if the same mechanism of deformation remains operative.

In the basic theory, the B term is a measure of the theoretical flow volume qA since $B = \sqrt{\frac{2}{3}} \frac{qA}{2kT}$. The computed flow volume for frozen Sault St. Marie clay investigated in this study is roughly of the order of magnitude of 10^5 to 10^6 A^3 ($1A^9 = 10^{-8}$ cm.) Flow volumes between 10^3 to 10^4 A^3 exist in steel and glass. Flow volume of asphalt ranges from 2×10^5 to 6×10^5 A^3 (Herrin and Jones, 1963). For comparison, a soil particle of 0.001 mm in diameter, a typical particle size in the Sault St. Marie clay, has a volume equal to 0.52×10^{12} A^3 . This would tend to indicate that the flow volume in question does not involve entire soil particles but rather contact areas between individual soil particles orice grains and soil particles.

The change in flow volume at a constant temperature and varied stress would then be explained in terms of the change in contact area.

If flow units involve molecules distributed along the contacts throughout the frozen mass, then a change in contact area would change the number

of these molecules per contact. Changes in contact area due to stress increase may be attributed to glide of soil particles at the contact or rotation of such particles with respect to initial position or both.

The B value also increases with increasing temperature. This is illustrated in Figure 6-5 where B is plotted against temperature for constant creep rates. Volume of flow units of most metals tend to increase slightly with temperature (Kauzmann, 1941). In the case of frozen soils, an increase in temperature results in increase of the unfrozen water accompanied with a change in the nature and area of contact. The increase in contact area with increasing temperature could be explained in terms of the interfacial energies at the contact. Figure 6-6 shows a simplified representation of a contact between two particles and adjacent ice grains.

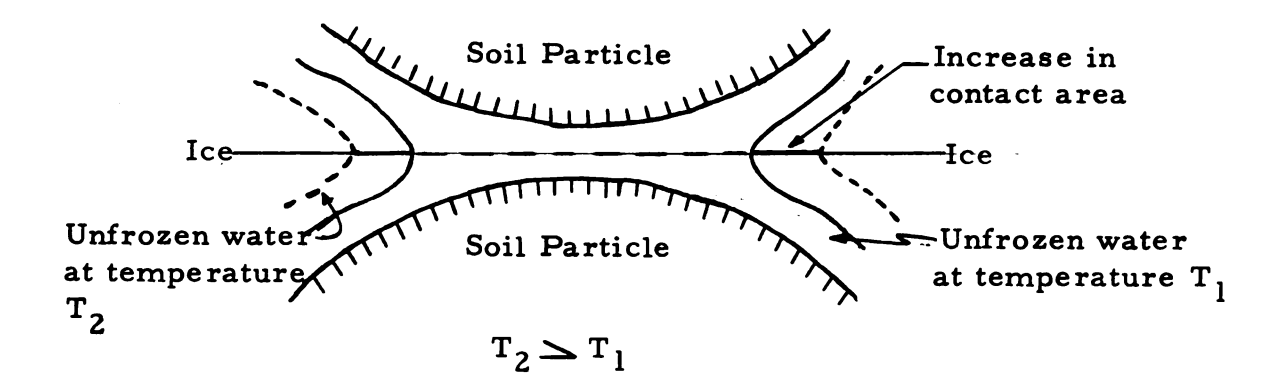


Figure 6-6. Simplified Representation of Contact Region Between Two Particles and Adjacent Ice Grains

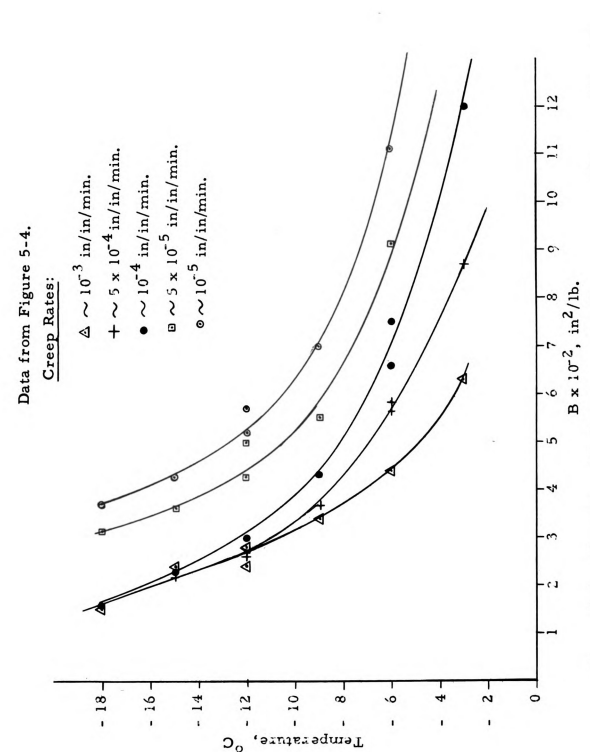


Figure 6-5. Variation of B Parameter with Temperature at Constant Creep Rates Sault St. Marie Clay

At temperature T_1 , there is a definite configuration of the water layer between soil particles and adjacent ice. At a temperature $T_2
ightharpoonup T_1$, the interfacial energy decreases moving the ice water interface to the outer region, thus increasing the area of contact involved in resisting deformation between soil particles.

It should be noted that the increase in unfrozen water with increase in temperature is accompanied with decrease in the strength of ice crystals (Tsytovich, 1963). This indicates that although contact area may increase due to increase in temperature, the bonding strength due to ice cementation decreases simultaneously.

It appears that the flow volume is restricted to that portion of the structure lying between contacts where contacts between individual particles or ice to soil particles would be involved. Thus, the flow units in question are most likely the water molecules held least tightly to the mineral surface. In other words, the water molecules (in liquid phase) farthest from the mineral surface are the most mobile.

The study of the effect of stress-strain history on the B parameter as shown in Figure 5-7a through 5-7e indicates strongly that B remains nearly the same at the same stress level irrespective of the stress-strain history. This behavior is in agreement with the general interpretation of B just presented.

The K Parameter

It has been shown in Chapter V that K of equation (5-2) is not a constant for the range of stresses and temperatures investigated in this study. K decreases with:

- (a) Decreasing stresses
- (b) Increasing strains, and,
- (c) Increasing temperatures as shown in Figure 5-2 and 5-4.

Figure 5-7a through 5-7e show that K is a history dependent parameter, unlike the B term which appears to be history independent. The parameter K may be written in an explicit form to include the energy temperature term as follows:

$$K = S e^{-\Delta F/RT}$$
 (6-1)

where S is a structure term, sensitive to stress history, temperature history, and the instantaneous values of stress and strain. The free energy of activation ΔF was defined in Chapter II. A change in K may be attributed to a change in S, ΔF or both. According to the rate process theory (equation 2-14) the S term is equivalent to $\frac{\sqrt{2\lambda_k} T}{\lambda_l}$ and since the change in T is relatively small in this study (270.3 K - 255.3 K), the S term would be essentially constant for the temperature range investigated if $\frac{2\lambda}{\lambda_l}$ equals unity. This is true only if the rate determining process or processes remain unchanged. This supports the idea that any change in the parameter K

is due primarily to a change in ΔF .

According to equation (2-16) and for the relatively high stress range investigated, the creep rate temperature relationship may be written as follows:

$$\ln \dot{\epsilon} = \ln S + BC - \frac{\Delta F}{R} (\frac{1}{T}) - \ln 2 \quad (6-2)$$

If S, B, and C are constants, then a plot of logarithm $\stackrel{\circ}{\epsilon}$ versus $\frac{1}{T}$ should be a straight line with slope $2\frac{\Delta F}{303R}$. Equation (6-2) is applied to part of the results presented in Figure 5-4 and 6-4. Figure 6-7 shows the logarithm of creep rate versus the reciprocal of temperature for a range of stresses (800 psi - 400 psi). In the high stress range, where data was derived from Figure 5-4, logarithm of creep rates versus $\frac{1}{T}$ are reasonably parallel lines. In the lower range of stress, where data was derived from Figure 6-4, the slope of the lines increases with decreasing stress. According to equation (6-2) the slope of these lines is a measure of ΔF since R is the gas constant. The value of ΔF in the high stress range (800 psi - 600 psi) is approximately 100 k cal/mole.

It should be pointed out that B is a function of temperature and stress, as shown in Figures 5-4 and 6-5. However, its variation is rather small in the region below -9°C at high stresses, such that B may be considered a constant. In addition to this, there is some question whether the S term would remain constant over the entire range, since the controlling mechanism (or mechanisms) of

deformation are known to change with decreasing stresses.

In order to supplement the stress versus free energy of activation results obtained by the stress reduction technique, several regular creep tests were performed under presumably constant structure conditions. Identical frozen samples were crept under a stress of 675 psi to a conventional strain of 9.0% for temperatures of -12°C, -15°C and -18°C. The temperature range investigated corresponds to the range where changes in unfrozen water are small as indicated in Figure (4-2). The assumption of a constant B is not too far off for the applied stress and temperature range chosen as shown by Figure (5-2) and (5-4).

Thus the use of identical samples crept under constant stress with identical stress history, compared at constant strain and almost identical unfrozen water content justifies the assumption of a constant S. It appears that all terms in equation (6-2) should be constants except T and $\hat{\epsilon}$.

Figure (6-8) shows the straight line relationship between $\ln \dot{\xi}$ and $\frac{1}{T}$, where T is determined on the absolute scale. From the slope of the straight line ΔF can be evaluated, thus

 $\Delta F = \text{slope x 2.303 x R}$

Where R = 1.987 cal per mole per degree centigrade

The estimated ΔF is 112 k cal/mole.

Another approach for evaluating the free energy of activation

involving duration of test is presented below (Dorn, 1954). This approach is based on the assumption that creep curves for the same stress and different temperatures, when plotted as a function of the logarithm of the time under test, are identical except for parallel displacement along the time axis. Consequently, the same total creep strains are obtained for identical values of

$$\ln t + \Psi(T) \tag{6-3}$$

where t is the duration of the test and Ψ is some function of the temperature T. But, since creep is a thermally activated process, the function $\Psi(T)$ might be replaced by $-\Delta F/RT$, where ΔF is the free energy of activation and R is the gas constant. Under such an assumption, the total creep strain, ϵ , would be given by the functional relationship.

$$\epsilon = f \left(t e^{-\Delta F/RT}\right)$$
, $\epsilon = constant$ (6-4)

In this event, the free energy of activation for creep of frozen soils could be determined from two creep tests conducted under the same stress at two different temperatures. If the time to reach the same strains at temperatures T_1 and T_2 are t_1 and t_2 respectively,

$$t_1 e^{-\Delta F/RT_1} = t_2 e^{-\Delta F/RT_2}$$
 (6-5)

and ΔF can be evaluated.

The data employed in the previous method of $\ln \dot{\xi}$ versus $\frac{1}{T}$ are used here for comparison purposes. For example, when t = 11 min.

at
$$-12^{\circ}$$
C and t = 127 min. at -15° C

$$\frac{11}{127} = e^{\Delta_i F(\frac{1}{RT_1} - \frac{1}{RT_2})}$$

$$\ln \frac{11}{127} = \Delta F \left(\frac{1}{RT_1} - \frac{1}{RT_2} \right) = \frac{\Delta F}{R} \left(\frac{-3}{6.749 \times 10^4} \right)$$

ln .08661 =
$$-\frac{\Delta F}{R}$$
 (4.445 x 10⁻⁵)

$$\frac{\Delta F}{R} = \frac{1.06243 \times 2.23026 \times 10^5}{4.445}$$

and $\Delta F = 1.987 \times .55035 \times 10^5 = 109.4 \text{ k cal/mole}$. Similarly, the other two values of ΔF are determined. Results of this method are shown in Table (6-1).

TABLE 6-1. Summary of Data on the Duration of Test Method for Determination of the Free Energy of Activation Under a Creep Stress of 675 psi (Frozen Sault St. Marie Clay)

Sample No.	Test Temperature				Average Time to Reach 9% Conventional Strain	F in k cal	/mole
A-2 (6) A-2 (7)	(1)	-12°C	ll min.	from (1) & (2)	109.4		
A-3(13)	(2)	-15 ⁰ C	127 min.	from (2) & (3)	83.0		
A-3(15)	(3)	-18°C	845 min.	from (3) & (1)	96.0		
				Average =	96.33		

The values of ΔF obtained at 675 psi by the logarithmic plot of creep rate versus $\frac{1}{T}$, along with the duration of test method, agree

well with results presented in Figure 6-7 for a comparable stress.

Figure 6-9 shows the observed free energy of activation versus axial stress for the range investigated.

Plots similar to Figure 6-9 have been shown for a variety of metals where the free energy of activation increases with decreasing applied stress (Osipov, 1964). With increasing stresses the observed values tend to reach a limiting ΔF , which is considered as a minimum ΔF for creep. It may be stated here that the so-called minimum ΔF for frozen Sault St. Marie clay is of the order of 100 k cal/mole. Results obtained by Dillon (in preparation) indicate an observed ΔF from 90-100 k cal/mole for the same stress and temperature range investigated in this study.

The observed $\triangle F$ may be due to single mechanism or several mechanisms operating simultaneously. If the mechanisms are operating in series (i.e., the operation of one depends on the operation of the others), the slowest mechanism is controlling; if they are in parallel, the fastest will be controlling. The particular mechanism (or mechanisms) which is controlling will depend on stress and temperature. Accordingly, for mechanisms in parallel, the strain rate may be given as follows: (Conrad, 1961).

$$\dot{\epsilon} = s_1 e^{-\Delta F_1/RT} + s_2 e^{-\Delta F_2/RT} + \cdots$$

where the observed $\Delta F = \Delta F_1 + \Delta F_2 + ----$

		3
		:
		;
		!

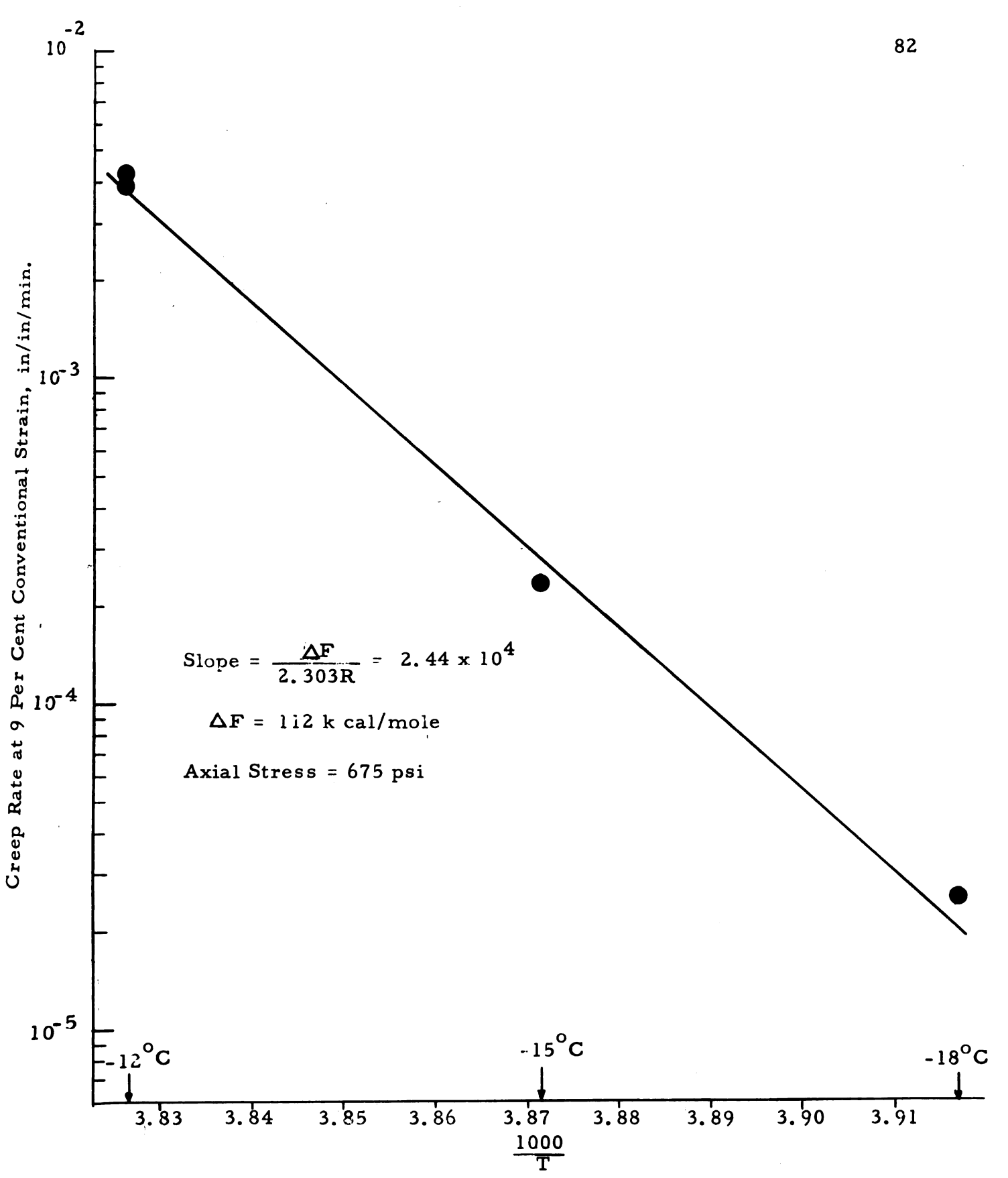
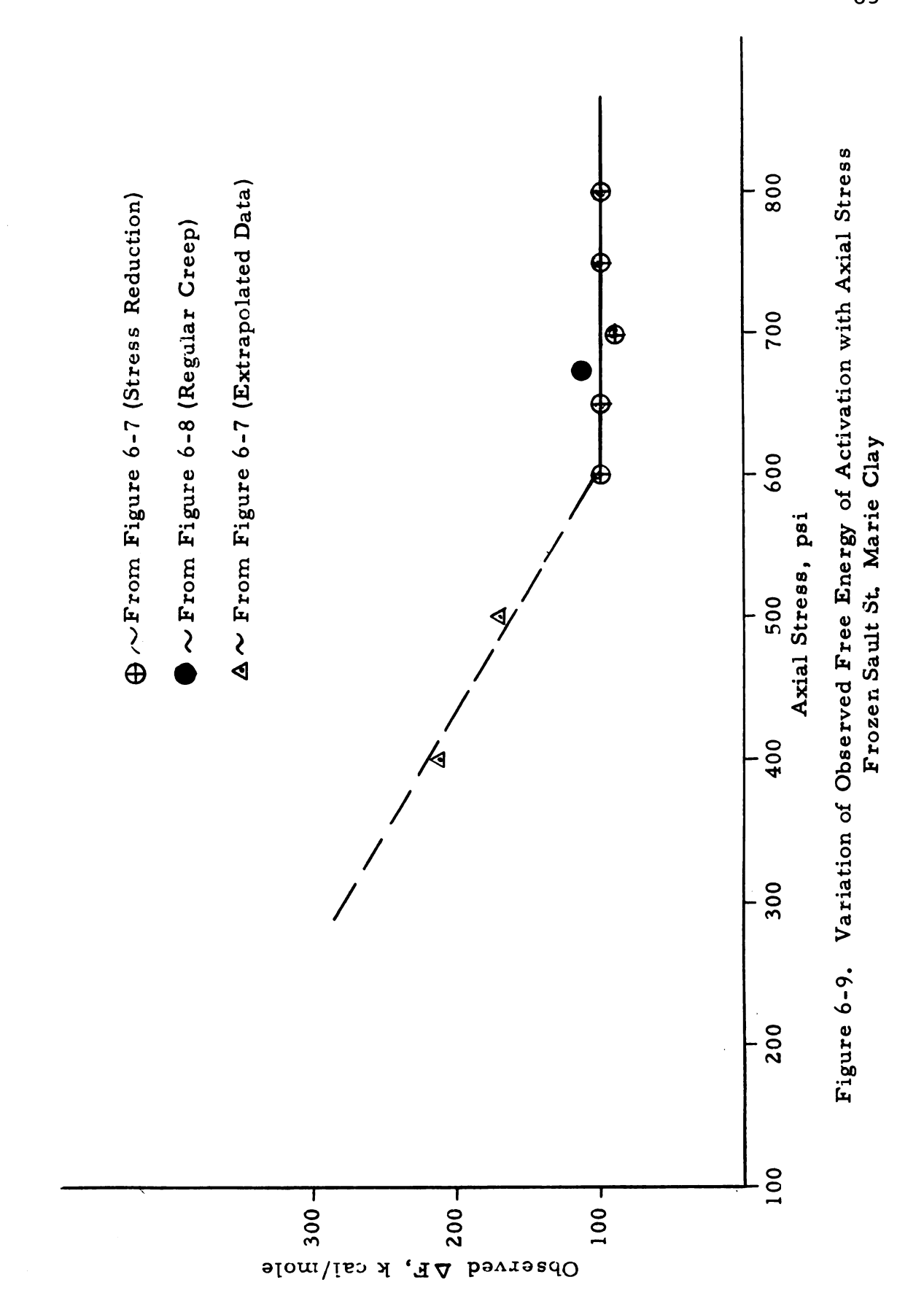


Figure 6-8. Creep Behavior of Frozen Sault St. Marie Clay - Evaluation of the Free Energy of Activation (ΔF) at 9 Per Cent Conventional Strain



CHAPTER VII

SUMMARY AND CONCLUSION

Creep behavior of frozen Sault St. Marie clay has been investigated over a range of stress and temperature. Duplicate frozen samples at constant initial density and moisture content, minimized initial structural differences during creep.

Stress reduction was applied in the steady-state region of creep and where changes in creep rate were relatively small. This technique permits the measurement of stress effect on creep rate under conditions of constant structure. The functional dependence of creep rate on applied stress has been approached from the point of view of the rate process theory.

The rate process equation, in the abbreviated form of $\dot{\epsilon}$ = K sinh B σ , has been applied to the experimental data in a range of high stress where it is approximated by $\dot{\epsilon} = \frac{K}{2} e^{B\sigma}$. The parameters B and K were determined from the creep rate $\dot{\epsilon}$ (in/in/min.), and the applied stress σ (psi). Figures 5-2 and 5-4 show the applied axial stress versus logarithm of creep rate over the range of stress and temperature investigated.

Experimental results show that B and K change with applied stress and temperature. The parameter B remains almost constant in the undamped creep region and increases with decreasing stresses

in the damped region. It increases with increasing temperatures, and seems to be independent of the stress history and depends only on the applied stress. Results indicate that K decreases with decreasing stresses, increasing strains, and increasing temperatures. The parameter K is also history dependent.

According to the theory, the change in B corresponds to the change in the flow volume. This can be interpreted in terms of the change in the area of contact corresponding to changes in applied stress and temperature. The K parameter contains in it the free energy of activation, and a structure factor. The decrease in K at presumably constant conditions of structure is attributed to the increase in the energy of activation. An observed free energy of activation equal to 100 k cal/mole was determined for the undamped region in the relatively low temperature region (below -9°C).

The separation of the two regions of creep (damped and undamped) by the critical stress was substantiated by creep data over a range of temperature (Figure 6-4). Critical stress corresponds to a creep rate of about 10⁻⁴ in/in/minute. It appears that critical stress is the long term strength that develops during the deformation process (Vialov, 1961). It is the net result of the strengthening and weakening mechanisms that operate during creep. At stresses below critical, the bond strength at the contact level increases with deformation. At stresses above critical, the bond

strength decreases with deformation leading to eventual break up of the bond.

The presentation of the data in the form shown in Figure 6-4 permits prediction of creep rates under known creep stress and temperature. The straight line relationship at constant creep rates (Figure 6-4) below -9°C, permits extrapolation of present data over a wider range of stress and temperature.

The creep behavior of frozen Sault St. Marie clay seems to be explained by the theoretical considerations suggested by the rate process theory. The theory appears to be quite applicable in the steady state region of creep at low temperatures.

BIBLIOGRAPHY

- Bowden, F. P. and Tabor, D. Friction and Lubrication of Solids, Clarendon Press, Oxford, 1954.
- Broms, B. B., and Yao, L. Y. C. "Shearing Strength of a Soil
 After Freezing and Thawing," Journal of Soil Mechanics
 and Foundation Division, ASCE, vol. 90, no. SM 4, July,
 1964.
- Burwell, J. T. and Rabinowicz, E. "The Nature of the Coefficient of Friction," <u>Journal of Applied Physics</u>, vol. 24, no. 2, 1953, pp. 136-139.
- Christensen, R. W. and Wu, T. H. "Analysis of Clay Deformation as a Rate Process," <u>Journal of Soil Mechanics and</u>
 Foundation Division, ASCE, vol. 90, no. SM 6, Nov., 1964.
- Conrad, H. "An Investigation of the Rate Controlling Mechanism for Plastic Flow of Copper Crystals at 90° and 170°K," Acta Metallurgica, vol. 6, 1958.
- Conrad, H. "Experimental Evaluation of Creep and Stress Rupture,"

 Chapter 8, Mechanical Behavior of Materials at Elevated

 Temperatures, Ed. by J. E. Dorn, McGraw-Hill Book

 Company, Inc., New York, 1961, pp. 149.
- Dillon, H. B. "Temperature Effect on Creep Rates of a Frozen Clay Soil," Unpublished Ph. D. Thesis, Michigan State University. (In preparation)
- Dorn, J. E. "The Spectrum of Activation Energies for Creep," Creep and Recovery, The American Society of Metals, Cleveland, Ohio, 1957, pp. 255-283.
- Dorn, J. E. "Some Fundamental Experiments on High Temperature Creep," <u>Journal of Mechanics and Physics of Solids</u>, vol. 3, 1954, pp. 85-116.
- Feltham, P. "The Plastic Flow of Iron and Plain Carbon Steels Above the A₃-Point," <u>Proc. Physical Society of London</u>, Section B, vol. 66, 1953.

- Fredrickson, J. W., and Eyring, H. "Statistical Rate Theory of Metals," Bulletin of the University of Utah, Bulletin no. 40 of the Utah Engineering Experiment Station, 1948.
- Glasstone, S., Laidler, K. J., and Eyring, H. The Theory of

 Rate Processes, McGraw-Hill Book Company, Inc., New
 York, 1941.
- Glen, J. W. "The Creep of Polycrystalline Ice," Proc. Royal Society of London, Ser. A, 228, 1955, pp. 519-538.
- Grim, R. E., Clay Mineralogy, McGraw-Hill Book Company, Inc., New York, 1953.
- Herrin, M., and Jones, G. E. "The Behavior of Bituminous Materials from the Viewpoint of the Absolute Rate Theory,"

 Proc. Association of Asphalt Paving Technologist, vol. 32, 1963, pp. 82-101.
- Jackson, K. A., and Chalmers, B. "Study of Ice Formation in Soils," (Arctic Construction and Frost Effects Laboratory, for office of the Chief of Engineers, Airfields Branch, Engineering Division, Military Construction, Technical Report No. 65, Nov, 1957.) U. S. Army Corps of Engineers, Boston, 1957.
- Jellinek, H. H. G., and Brill, R. "Viscoelastic Properties of Ice,"

 Journal of Applied Physics, vol. 27, no. 10, 1959, pp.

 1198-1209.
- Kauzmann, W. "Flow of Solid Metals from the Standpoint of the Chemical-Rate Theory," <u>Trans. American Institute of Mining and Metallurgical Engr.</u>, vol. 143, pp. 57-83, 1941.
- Kennedy, A. J. Processes of Creep and Fatigue in Metals, John Wiley and Sons, Inc., New York, 1963.
- Lambe, T. W. "A Mechanistic Picture of Shear Strength in Clay,"

 <u>American Society of Civil Engineers Research Conference on</u>

 Shear Strength of Cohesive Soils, 1960, pp. 555-580.
- Leonards, G. A. "Strength Characteristics of Compacted Clays," Trans. ASCE, vol. 120, 1955.

- Mitchell, J. K. "Shearing Resistance of Soils as a Rate Process,"

 Journal of Soil Mechanics and Foundation Division, ASCE,
 vol. 90, SM 1, 1964.
- Mitchell, J. K. and Campanella, R. G. "Creep Studies on Saturated Clays," ASTM Symposium on Laboratory Shear Testing of Soils, Ottawa, Canada, 1963.
- Nadai, A. Theory of Flow and Fracture of Solids, vol. 2, McGraw-Hill Book Company, Inc., New York, 1963.
- Osipov, K. A. Activation Processes in Solid Metals and Alloys, American Elsevier Publishing Company, Inc., New York, 1964.
- Sherby, O. D., Frenkel, J., Nadeau, J., and Dorn, J. E.

 "Effect of Stress on the Creep Rates of Polycrystalline
 Aluminum Alloys Under Constant Structure," <u>Trans.</u>,

 American Institute of Mining and Metallurgical Engineers,
 vol. 200, 1954, pp. 275-279.
- Tsytovich, N. A. "The Instability of the Mechanical Properties of Frozen Grounds," International Conference on Permafrost, Purdue University, Lafayette, Indiana, Nov., 1963.
- Vialov, S. S. "Rheology of Frozen Grounds," International Conference on Permafrost, Purdue University, Lafayette, Indiana, Nov., 1963.
- Vialov, S. S. "Mechanism of Rheological Processes," Chapter 2, The Strength and Creep of Frozen Soils and Calculations for Ice-Soil Retaining Structures, Edited by S. S. Vialov, 1961, U. S. Army CRREL Translation 76.
- Williams, P. J. "Suction and its Effects in Unfrozen Water of Frozen Soils," International Conference on Permafrost, Purdue University, Lafayette, Indiana, Nov., 1963.
- Wu, T. H., Loh, A. K., and Malvern, L. E. "Study of Failure Envelope in Soils," <u>Journal of Soil Mechanics and Foundation</u> Division, ASCE, vol. 89, no. SM 1, Feb., 1963.



I. CREEP DATA FOR SOIL CAKE NO. A-1 TABLE Molded Moisture Content = 25.68% Molded Dry Density = 98.04 lb/cu. ft.

		-			
Time	True Strain	Time	True Strain	Time	True Strain
(Min.)	(%)	(Min.)	(%)	(Min.)	(%)
SAMPL	E NO. A-1 (9)	80	11.70	30	7.80
Axial St	ress = 625 psi	81	11.72	35	8. 33
	Moisture	82	11.74	40	8.83
	nt = 25.78%	84	11.79	45	9. 32
		90	11.93	50	9.78
1/2	. 02	100	12.14	55	10.30
1-1/2		115	12, 43	60	10.78
2	. 28	125	12.63	65	11.24
2-1/2		135	12.85	67	11.45
3	1.30	165	13.36 .	69-1/	4 11.65
4	2.28				
5	2.76	SAMPLE	NO. A-1 (16)	Stress	Decrease=
6	3.08	Axial Str	ess = 625 psi	50 psi at	€ = 11.65%
7	3.38	$\mathbf{F}_{\mathtt{inal}}$	Moisture	•	•
8	3.61	Conter	nt = 25.96%	71	11.69
9	3.85			73	11.74
10	4.05	1/	2 .10	75	11.80
12	4.52	1	. 39	77	11.86
14	4.91	1-1/		80	11.92
16	5. 29	2	2.03	82	11.97
18	5.61	2-1/	2 2.27	85	12.05
20	5.92	3	2.61	87	12.09
22	6.23	4	3.09	90	12.18
24	6.53	5	3.43	95	12.31
26	6.82	6	3.73	100	12.43
28	7.11	7	3.99	105	12.54
30	7.36	8	4.24	110	12.66
35	8.01	9	4.49	115	12.80
40	8.57	10	4.73	120	12.91
45	9.05	11	4. 96		
50	9.49	12	5. 16	SAMPLE	NO. A-1 (17)
55	9.89	13	5.34	Axial St	ress = 625 psi
60	10.30	14	5.54	Fina	l Moisture
65	10.73	16	5.88	Conte	nt = 25.63%
77	11.65	18	6. 22		
		20	6.49	1/	
Stress Decrease =		22	6.79	1	. 31
50 psi at	€= 11.65%	24	7.06	1-1/	
70	11 /0	26	7.31	2	1.48
79	11.69	28	7. 56	2-1/	2 2.32

TABLE I (Continued)

Time (Min.) SAMPLE NO.	True Strain (%) A-1(17) Contd.
3	2.65
4	3. 19
5	3.60
6	3. 96
7	4. 29
8	4.58
9	4.84
10	5.10
11	5.32
12	5.55
14	5.92
16	6.30
18	6.66
20	6.99
22	7.32
24	7.62
26	7.92
28	8.21
30	8.49
35	9.15
40	9.73
45	10.30
50	10.82
55	11.35
58	11.62
58-1/2	11.65
Stress 1	Decrease =
25 psi at	ϵ = 11.65%

•		•
59	11.74	
60	11.79	
62	11.90	
65	12.06	
67	12.17	
70	12.32	
72	12.44	
75	12.60	
77	12.71	
80	12.87	
85	13.15	
90	13.42	
95	13.70	

TABLE II. CREEP DATA FOR SOIL CAKE NO. A-2

Molded Moisture Content = 26.02% Molded Dry Density = 98.08 lb/cu. ft.

Time	True Strain	Time	True Strain	Time	True Strain
(Min.)	(%)	(Min.)	(%)	(Min.)	(%)
SAMPLE	NO. A-2(1)	79	11.87	30	12.17
	ess = 625 psi	81	11.88	32	12.27
	Moisture	83	11.89	34	12.36
	t = 25.72%	85	11.90	36	12.44
		92	11.96	38	12.51
1/2		95	11.98	40	12.58
1	.20	100	12.05	42	12.65
1-1/2		105	12.09	44	12.71
2	1.55	110	12.15	4 6	12.78
2-1/2		120	12.26	48	12.85
3	2.44			50	12.94
4	2.99	SAMPLE	NO. A-2 (6)	52	13.01
5	3. 43	Axial Stre	ess = 675 psi	57	13.17
6	3.74	Final N	Moisture	60	13.25
7	4.01	Content	= 25.70%	62	13.33
8	4.25	1/2	. 39	65	13.43
9	4.47	1, 2	1.28	68	13.50
10	4.81	1-1/2		70	13.58
12	5.22	2	2.82	70	13. 30
14	5.69	2-1/2		SAMDLE	NO. A-2(7)
16	6.06	3	4.66		ess = 675 psi
18	6.43	4	5. 59		Moisture
20	6.76	5	6.30		t = 25.70%
22	7.02	6		Conter	10 - 25. 70%
24	7.31	7	6.86	1/2	. 36
28	7.80	8	7.39	1	.84
35	8.58	9	7.90	1-1/2	1.41
40	9.00		8.41	2	2.94
45	9.48	10	8.90	2-1/2	3. 45
50	9.87	12	9.71	3	
55	10.29	14	10.37		4. 58
60	10.67	16	10.89	4	5 . 4 5
65	11.05	18	11.44	5	6.09
70	11.43	18-3/4	11.65	6	6.64
72	11.58	Stress	Decrease=	7	7.21
73	11.64	75 psi at	€ = 11.65%	8	7.79
73-1/4		-		9	8. 29
		20	11.81	10	8.74
	Decrease =	22	11.84	11	9.13
_	€ = 11.65%	24	11.92	12	9.49
75	11.84	26	12.00	14	10.16
77	11.86	28	12.08	16	10.80

TABLE II (Continued)

Time	True Strain	Time	True Strain	Time	True Strain
(Min.)	(%)	(Min.)	(%)	(Min.)	(%)
SAMPLE	A-2 (7) Contd.				
		7	6.68	9	7.70
18	11.36	8	6.81	10	7.95
19	11.62	9	6.94	11	8.22
19+	11.65	10	7.11	12	8 . 4 6
		11	7.25	13	8.64
Stres	s Decrease =	12	7.38	14	8.85
50 psi at	€ = 11.65%	13	7.49	15	9.04
_		14	7.62	16	9.21
21	11.84	15	7.73	17	9.40
22	11.91	17	7.96	18	9.62
23	11.99	19	8.20	19	9.82
24	12.07	21	8.39	20	9.98
26	12.23	23	8.60	22	10.29
28	12.37	25	8.81	24	10.60
30	12.53	27	9.00	26	10.91
32	12.69	29	9.19	28	11.19
34	12.84	31	9.38	30	11.47
36	13.00	35	9.73	35	12.14
38	13.16	43	10.39	37	12.40
40	13.30			40	12.77
45	13.70	SAMPLE	NO. A-2 (9)	42	13.03
47	13.86	Axial Str	ess = 675 psi	45	13.43
		Final	Moisture	47	13.68
SAMPLE	NO. A-2(8)	Content	: = 25.82%	50	14.06
Axial Str	ess = 675 psi				
Fina!	Moisture	1/2	2 .48	SAMPLE	NO. A-2(10)
Conte	nt = 25.46%	1	. 99	Axial Str	ess = 675 psi
		1-1/2	1.81	Final	Moisture
1/2	. 50	2	2.88	Conte	nt = 25.76%
1	.74	2-1/2	4.00		
1-1/2	1.86	3	4.76	1/2	. 48
2	2.88	3-1/2	2 5.35	1	1.09
2-1/2	3.91	4	5.83	1-1/2	2.02
3	4.61	4-1/2	2 6.19	2	3.22
3-1/2	5.00			2-1/2	4. 29
4	5.52		Decrease =	3	4.95
4-1/2	5. 88	50 psi at	ϵ = 6.19%	4	5.88
5+	6.19			5	6.54
Stress	Decrease =	5-1/2		6	7.16
	$\epsilon = 6.19\%$	6	6.88	7	7.73
_		7	7. 12	8	8.34
6	6.56	8	7.40	9	8.81

TABLE II (Continued)

Т: •	T St	T:	Tuna Startin	m:	T St
Time	True Strain	Time	True Strain	Time	True Strain
(Min.)	(%)	(Min.)	(%)	(Min.)	(%)
SAMPLE	A-2(10)Contd.	2 1/2	4 05	1	.63
10	0.20	2-1/2	4.05		
10	9.28	3	4.79	1-1/2	1.91
10-1/2	9.43	4	5.74	2	2.81
a .	_	5	6. 42	2-1/2	3. 21
	Decrease =	6	7.04	3	3.50
75 psi at	€ = 9.43%	7	7. 59	4	3.99
		7-1/2	7.85	5	4.41
12	9.74	8	8.10	6	4.75
13	9.80	8-1/2	8. 32	7	5.05
14	9.88	9	8.53	8	5.31
15	9.98	9-1/2	8.74	9	5.54
16	10.05	10	8.96	10	5. 76
17	10.12	10-1/2	9.17	12	6. 16
18	10.19	11	9.36	14	6.49 .
20	10.32	11-1/4	9.43	16	6.85
22	10.46			18	7.17
24	10.59	Stress	Decrease =	20	7.4 6
26	10.70	50 psi at	€ = 9.43%	22	7.72
28	10.85	12-1/2	9.74	24	-8.00
30	10.96	13	9. 80	26	8.23
32	11.08	13	9.93	28	8.45
34	11.19	15	10.05	30	8.68
36	11.33	16		32	8.89
38	11.47		10.17	34	9.09
4 0	11.59	17	10.32	4 0	9.67
42	11.70	18	10.44	4 5	10.07
44	11.82	20	10.71	50	10.41
46	11.95	22	10.96	55	10.78
4 8	12.07	24	11.18	60	11.11
50	12.18	26	11.43	65	11.40
59	12.66	28	11.63	67	11.50
62	12.83	30	11.89	68	11.54
65	13.00	32	12.09	69	11.59
	23.00	34	12.33	70+	11.65
SAMPLE	NO. A-2(11)	36	12.54		
	ess = 675 psi	38	12.74	Stress	Decrease =
	Moisture	40	12.93		€ = 11.65%
	nt = 25.53%	CAMDIE	NO 4 2/12\	is por ac	(11.05/0
Conte	11t - 6J. 33 yo		NO. A-2(12) sss = 600 psi	71-1/2	11.75
1/2	22		Moisture	77	11.77
1/2 l	. 23		t = 25.70%	80	11.79
	. 78		. ••	82	11.80
1-1/2	1.71	1/2	. 32	85	11.82
2	2.80	1/2	. 34	0.5	11,02

TABLE II (Continued)

Time	True Strain	Time	True Strain	Time	True Strain
(Min.)	(%)	(Min.)	(%)	(Min.)	(%)
•	A-2(12) Contd.	(141111. /	(70)	(141111. /	(70)
OAWII DD	H-2(12) Conta.	47	10.85	7	5.09
87	11.83	49	11.00	8	5.32
90	11.87	53	11.29	9	5, 53
92	11.88	56	11.51	10	5.72
9 4	11.89	57	11.56	12	6.07
98	11.92	58	11.62	14	6.38
102	11.95	58+	11,65	16	6.69
110	12.01			18	6.96
120	12.09	Stress	Decrease =	20	7.21
130	12.16	50 psi at	€ = 11.65%	22	7.45
		-		24	7.67
SAMPLE	NO. A-2(13)	59-1/2	11.72	26	7.88
	ess = 600 psi	62	11.74	28	8.06
	Moisture	63	11.75	30	8.26
Conter	nt = 25.55%	64	11.77	35	8.66
	·	65	11.78	40	9.06
1/2	. 43	67	11.81	45	9.39
1	1.08	69	11.86	50	9.70
1-1/2	1.92	73	11.95	55	10.00
2	2.85	77	12.04	60	10.27
2-1/2	3.37	80	12.09	65 70	10.52
3	3.76	85	12.18	70 75	10.74
4	4. 36	90	12, 25	75 77	11.00 11.09
5	4.79	95	12.33	80	11.22
6	5. 17	100	12.40	82	11.31
7	5.47	105	12.48	85	11.43
8	5.75	110	1 2. 56	87	11.51
9	6.03			89	11.60
10	6.24			90+	11.65
12	6.67		NO. A-2(16)	Stress	Decrease =
14	7.05	Axial Stre	ss - 675 psi	50 psi at	
16	7.42		Moisture	-	•
18	7.74	Content	: = 25.68%	92	11.66
20	8.06			94	11.68
22	8.35	1/2	. 53	96	11.69
24	8.60	1	1.35	98	11.71
26	8.84	1-1/2	2.26	100	11.72
28	9.07	2	2.81	103	11.74
30	9.29	2-1/2	3.23	107	11.79
32	9.46	3	3.57	110	11.82
35	9.82	4	4. 09	115	11.88
40	10.28	5	4.50	120	11.91
45	10.67	6	4. 79	130	11.99

TABLE II (Continued)

Time	True Strain	Time	True Strain	Time	True Strain
(Min.)	(%)	(Min.)	(%)	(Min.)	(%)
-	NO. A-2(17)	•	NO. A-2 (20)	(141111.)	(/0)
	ess = 600 psi		ess = 600 psi	71-3/4	9.44
	Moisture		Moisture	Stragg T	Decrease =
	nt = 25.58%		nt = 25.54%		
Conte	III - 25. 5670	Oome	III - 23. 34/0	ou psi at	€ = 9.44%
1/	2 .32	1/2	. 35	73	9.48
1	1.00	1	1.08	74	9.50
1-1/	2 1.94	1-1/2	2.04	76	9.52
2	2.47	2	2.76	78	9.54
2-1/	2 2.86	2-1/2	3.13	80	9.56
3	3.13	3	3.38	82	9.59
4	3.54	4	3.86	84	9.61
5	3.86	5	4.20	86	9.63
6	4.11	6	4.48	88	9.65
7	4.33	8	4.92	90	9.67
8	4.54	10	5.30	93	9.71
9	4.72	12	5.65	95	9.73
10	4.91	14	5.95	100	9.78
12	5.22	15	6.08	105	9.82
14	5.48	15-3/4	6.19	110	9.87
16	5.73			115	9.91
18	5.98	Stress 1	Decrease =	120	9.95
19	6.12	25 psi at	€ = 6.19%	125	9.99
20	6.19				
		17	6.29		NO. A-2 (21)
Stress	Decrease =	18	6.40		ess - 600 psi
75 psi at	€= 6.19%	19	6.50	Final	Moisture
		20	6.56	Conten	t = 25.40%
22	6.21	22	6.74		
23	6.22	24	6.94	1/2	. 35
24	6.24	26	7.10	1	1.03
25	6.26	28	7.23	1-1/2	1.92
27	6.29	30	7.36	2	2.42
29	6.34	35	7.67	2-1/2	2.73
32	6.39	40	7.97	3	2.97
35	6.4 5	45	8.20	4	3.40
38	6.52	50	8.44	5	3.70
40	6.55	55	8.65	6	3.96
45	6.66	60	8.95	7	4.20
50	6.74	65	9.16	8	4.41
55	6.83	69	9.31	9	4.58
60	6.94	70	9.34	10	4.75
65	7.02	71	9.40	12	5.07

TABLE II (Continued)

			,		
Time	True Strain	Time	True Strain	Time	True Strain
(Min.)	(%)	(Min.)	(%)	(Min.)	(%)
SAMPLE	A-2(21) Contd.	115	9.76		
	, , , , , , , , , , , , , , , , , , , ,	120	9.83		
14	5.33	125	9.88		
16	5. 59	130	9.94		
18	5.86		, , , -		
19	5.96				
20	6.08				
21	6.19				
Stress	Decrease =				
25 psi at	€ = 6.19%				
22	6.34				
23	6.42				
25	6.55				
27	6.70				
29	6.83				
33	7.07				
35	7.19				
40	7.45				
45	7.72				
50	7.95				
55	8.16				
60	8.37				
65	8.56				
70	8.75				
75	8.92				
80	9.08				
85	9.22				
88	9.31				
90	9.36				
92	9.43				
	Decrease =				
25 psi at	€ = 9.43%				
93	9.46				
94	9.48				
95	9.49				
97	9.52				
101					

101

105

108

9.57

9.63

9.66

TABLE III. CREEP DATA FOR SOIL CAKE NO. A-3

Molded Moisture Content = 26.33% Molded Dry Density = 98.09 lb/cu. ft.

Time	True Strain	Time	True Strain	Time	True Strain
(Min.)	(%)	(Min.)	(%)	(Min.)	(%)
(141111. /	(/0 /	(141111.)	(70)	(141111. /	(707
SAMPLE	NO. A-3(1)	425	3.03	3	1.39
Axial Str	ess = 400 psi	535	3.23	4	1.58
Final	Moisture	560	3.27	5	1.72
Conter	t = 25.93%	1150	3.88	6	1.86
		1355	4.00	7	1.97
1/2	. 32	1440	4.03	8	2.09
1	.86	1560	4.08	9	2.19
1-1/2	1.00	1850	4.20	10	2.30
2	1.06	2635	4.41	12	2.49
2-1/2	1.11	2875	4. 45	14	2.64
3	1.15	3200	4,50	16	2.72
4	1.19	3370	4.52	18	2.93
5	1.24	4125	4.64	20	2.99
6	1.26			22	3.18
7	1.31	Stress	Decrease =	24	3.29
8	1.33	40 psi at	€ = 4. 64%	26	3.42
9	1.35	-	•	28	3.51
10	1.39	4 365	4.64	30	3.61
11	1.41	4830	4.65	35	3.85
13	1.45	6120	4.67	40	4.05
15	1.47	7155	4.68	45	4.26
17	1.50	7795	4.69	50	4.44
19	1.52	8820	4.70	55	4.63
21	1.55			65	4.90
23	1.57	Sample	Unloaded	75	5.17
25	1.59	_	= 4.70%	85	5.42
27	1.61	Sample	Recovered	120	6.12
30	1.64	Under Ze	ero Stress to	135	6.39
40	1.71	€= 4.	21% and was	150	6.62
50	1.79	Subjecte	d to a Second	165	6.85
60	1.85	-	of Loading	185	7.16
70	1.90	•	cial Stress =	205	7.43
90	2.00	60	00 psi	225	7.71
120	2.14		•	26 5	8.16
150	2.26	1/2	.21	295	8.51
180	2.37	1	. 58	305	8.62
255	2.60	1-1/2	. 96	325	8.86
325	2.79	2	1.14	340	9.06
375	2.92	2-1/2	1.28	350	9.18

TABLE III (Continued)

				 .	
Time	True Strain	Time	True Strain	Time	True Strain
(Min.)	(%)	(Min.)	(%)	(Min.)	(%)
CAMDIE	A-3(1) Contd.	6	1.63	1850	7.96
SAMPLE	7 A-3(1) Conta.	7	1.69	1925	7.97
360	9.29	8		2690	8.08
370	9.40	9	1.75	2830	8.10
	9. 40 9. 43	10	1.78	2965	8.11
371	7. 43	10	1.83	3380	8.16
Stross	Decrease =	14	1.90 1.97	4100	8.23
40 psi at	_	16	2.03	4510	8.26
•	13.60% with	18	2.03	4780	8.28
• •	ct to Initial	20		5690	8.35
-	ing Cycle	22	2.14	30 70	0. 33
Load	ing Cycle	24	2.20 2.27	SAMDIE	NO. A-3(3)
373	9 . 4 8	24 26			ss = 675 psi
375	9. 49		2.31		Moisture
380	9. 4 9	28	2.36		t = 26.04%
385	9.50 9.52	30 40	2.40	Conten	l = 20. 0 1 /0
390	9.54	4 0	2.61	1/2	. 34
400	9. 57	50 70	2.81	1 1 2	1.02
420	9.65	70	3. 16	1-1/2	2.05
		80	3.31	2	3.19
440 465	9.73	130	3.97	2-1/2	3. 98
	9.84	160	4.29	3	4.50
4 90	9.94	170	4.40	4	5.30
510 1270	10.02	240	4. 95	5	
_	12.41	270	5. 15	6	5.95 6.47
1490	13.27	290	5.27	7	
1520	13.43	320	5.44		7.02
1550	13.60	430	5.90	8	7.54
1605	13.96	445	5.95	9	8.02
1665	14.27	460	6.01	10	8.47
CAMPIE	' NIO A 2/2\	490	6.15	11	8.88
	NO. A-3(2)	1210	7.36	12	9.25
	ress = 475 psi	1270	7.44	12-1/2	9.43
	Moisture	1350	7.52	C4	D
Conte	nt =	1435	7.59		Decrease =
1/2	27	1470	7.63	40 psi at	€ = 9.43%
, 1/2		1530	7.67	1.2	0.55
l 1 1/2	. 92	1560	7.70	13	9.55
1-1/2		1590	7.73	14	9.67
2	1.26	1630	7.75	15 16	9 . § 0
2-1/2		1670	7.80	16	9.99
3	1.41	C4	Decrease =	17	10.16
4	1.51			18	10.32
5	1.58	by psi at	€ = 7.80%	19	10.53

TABLE III (Continued)

Time	True Strain	Time	True Strain	Time	True Strain
(Min.)	(%)	(Min.)	(%)	(Min.)	(%)
SAMPLE	A-3(3) Contd.	Stress	Decrease =	15	4.06
		35 psi at	$\epsilon = 16.25\%$	20	4.47
20	10.69			25	4.81
21	10.86	177	16.26	41	5.75
22	11.02	180	16.29	60	6.60
23	11.17	185	16.31	90	7.61
24	11.32	200	16.42	105	7.99
25	11.47	290	17.10	125	8.40
26+	11.65	325	17.38	135	8.59
		350	17.60	145	8.78
Stress	Decrease =	400	18.03	155	8.95
37 psi at	€ = 11.65%			175	9.21
		Stress	Decrease =	190	9.37
27	11.79	35 psi at	€ = 18.03%	196	9.43
28	11.83				
29	11.91	405	18.03	Stress 1	Decrease =
30	11.97	430	18.07	40 psi at	€ = 9.43%
35	12.25	445	18.11		
40	12.53	625	18.52	197	9.44
45	12.82	1420	20.06	315	9.61
50	13.16	1540	20.53	375	9.72
55	13.44	1570	20.83	505	9.88
57	13.58			565	9.96
62-1/2	13.93	SAMPLE	NO. A-3(10)	1195	10.54
		Axial Str	ess = 525 psi	1245	10.58
Stress	Decrease =	Final	Moisture	1340	10.66
36 psi at	€ = 13.93%	Conter	nt = 25.12%	1440	10.74
64	13.98	1/2	.18	Stress 1	Decrease =
67	14.04	1	. 76	40 psi at	€ = 10.74%
70	14.08	1-1/2			
77	14.21	2	1.90	1442	10.80
80	14.28	2-1/2	2.31	1740	10.83
86	14.40	3	2.51	1985	10.84
90	14.46	4	2.80	2625	10.89
115	15.01	5	2.98	2985	10.94
135	15.42	6	3.14	3585	10.97
150	15.71	7	3.27	4095	11.00
160	15.91	8	3.39	4 755	11.01
165	16.02	9	3.51	5520	11.07
170	16.15	10	3.61	5895	11.08
170-1/2	16.25	12	3.81	7155	11.14

TABLE III (Continued)

Time	True Strain	Time	True Strain	Time	True Strain
(Min.)	(%)	(Min.)	(%)	(Min.)	(%)
(141111.)	(/0 /	(141111.)	(70)	(141111.)	(70)
SAMPLE	A-3(10)Contd.	8975	12.09	5	3.46
	,	9005	12.21	6	3.67
Stress	Decrease =	9050	12.32	7	3.85
40 psi at	= 11.14%	9080	12.41	8	4.03
		9110	12.50	9	4.18
9795	11.14	9140	12.58	10	4.31
10235	11.15	9860	14.08	12	4.54
10865	11.16	9890	14.12	14	4.76
		9920	14.16	16	4.95
Left Unde	er = 405	9985	14.25	18	5. 14
	Long Time.	9990	14.26	20	5.31
	Increase =			22	5.47
40 psi at	= 11.17%	Stress	Increase =	24	5.63
-		40 psi at	= 14.26%	26	5.77
0	11.17			28	5. 92
1550	11.17	9995	14.34	30	6.07
2960	11.22	10000	14.38	40	6.73
4130	11.23	10015	14.53	50	7.38
4790	11.24	10030	14.63	60	7.95
5540	11.26	10040	14.71	84	9. 26.
6320	11.27	10075	14.99	87+	9.43
6980	11.28	10080	15.02		•
7115	11.28			Stress	Decrease =
		Stress	Increase =	40 psi at	= 9.43%
Stress	Increase =	40 psi at	= 15.02%	-	
40 psi at	= 11.28%			88	9.50
		10085	15.21	91	9.56
7160	11.34	10095	15.49	97	9.73
7190	11.35	10100	15.64	105	9. 95
7310	11.40	10105	15.77	120	10.37
7370	11.42	10110	15.90	135	10.85
7610	11.52			150	11.32
7715	11.54		NO. A-3(4)	155	11.47
8405	11.83		ess = 800 psi	160	11.63
8615	11.91		Moisture	161	11.65
8780	11.96	Conter	nt = 25.56%		
8960	12.02			Stress	Decrease =
8965	12.06	1/2	. 39	40 psi at	= 11.65%
C 4 -	T	1	. 92		_
Stress 40 psi at	Increase = = 12.06%	2	2. 37	162	11.68
10 per at	- 12.00/0	2-1/2	2.68	165	11.71
8975	12.09	3 4	2.90 3.20	170 175	11.78 11.86

TABLE III (Continued)

.	—				
Time	True Strain		True Strain	Time	True Strain
(Min.)	(%)	(Min.)	(%)	(Min.)	(%)
SAMPLE	A-3(4) Contd.	20	3.26	1595	9.07
	11-3(1) Conta.	22	3.35	1820	9.18
180	11.92	24	3.41	1910	9.22
190	12.05	26	3.49	2780	9.59
200	12.21	28	3.55	2920	9.64
215	12.41	30	3.62	2,20	7.01
285	13, 54	35	3.79	Stress	Decrease =
300	13.79	55	4.31		<i>E</i> = 9.64%
305	13.89	110	5.36	To psi at	C - 7.0470
307	13.93	140	5.87	3260	9.65
301	13. 73	170	6.28	3380	9.66
Stress	Decrease =	190	6.55	4340	9.72
	$\epsilon = 13.93\%$	210	6.82	5450	9.76
40 par ac	- 13.75/0	230	7.05	6320	9.78
310	13.94	240	7.15	0320	7.10
315	13. 96	250	7.21	SAMPLE	NO. A-3(15)
330	14.08	253	7.26		ess = 675 psi
345	14.20	2 33	1.20		Moisture
360	14.32	Stress De	ecrease =		t = 25.89%
375	14.46		E = 7.26%	Conton	c = 23.0770
3.3	11. 10	ro por ac	(- 1, 20 / 0	1/2	. 17
SAMPLE	E NO. A-3(5)	255	7.32	1	.67
Axial St	ress = 700 psi	265	7.33	1-1/2	1.27
Fina!	Moisture -	270	7.34	2	1.61
Conte	nt = 26.08%	275	7.35	2-1/2	1.79
		285	7.40	3	1.85
1/2	. 35	370	7.67	4	1.98
1	. 88	420	7.85	5	2.07
1-1/2	1.51	510	8.13	12	2.47
2	1.76	530	8. 19	20	2.76
2-1/2	1.91	550	8.24	30	3.02
3	2.02	570	8.29	50	3.48
4	2.18	582	8.34	120	4.55
5	2.33			180	5.35
6	2.44	Stress De	ecrease =	345	6.96
7	2.52	40 psi at	€ = 8.34%	410	7.45
8	2.61			465	7.80
9	2.69	583	8.38	505	8.06
10	2.75	605	8.38	630	8.68
12	2.88	1235	8.86	1265	10.55
14	2.98	1310	8.89	1305	10.65
16	3.09	1370	8.94		
18	3.17	1430	8.97	1385	10.81

TABLE III (Continued)

Time	True Strain	Time	True Strain	Time	True Strain
(Min.)	(%)	(Min.)	(%)	(Min.)	(%)
				C4	- D
SAMPLE	A-3(15)Contd.	10200	14.00		S Decrease =
		10245	14.06	40 psi at	$\epsilon \in 10.54\%$
	Decrease =	10315	14.47	25	10.50
40 psi at	$\epsilon = 10.81\%$			35	10.59
			NO. A-3 (8)	37	10.65
1385	10.84		ess = 750 psi	40	10.73
1535	10.94		Moisture	42	10.83
1635	10.99	Conter	at = 25.74%	45	10.94
1875	11.16			47	11.00
2105	11.29	1/2	. 37	48	11.05
		1	1.04	49	11.08
Stress	Decrease =	1-1/2	1.83	49-1/3	11.09
40 psi at	€ = 11.29%	2	2.88	_	_
		2-1/2	3.87		Decrease =
2720	11.35	3	4.22	40 psi at	€ = 11.09%
4955	11.59	5	5.37		
6185	11.71	6	5.78	50	11.09
		7	6.15	51	11.10
Stress 1	Increase =	8	6.48	53	11.14
40 psi at	$\epsilon = 11.71\%$	9	6.79	60	11.23
		10	7.07	66	11.32
6245	11.74	11	7.33	75	11.44
6285	11.77	12	7.57	80	11.51
7045	12.02	14	8.03	85	11.57
7225	12.10	16	8.48	90	11.64
7345	12.14	17	8.71	90-1/2	11.65
7655	12.21	18	8.94		
8445	12.41	19	9.13		Decrease =
		20	9.33	40 psi at	€ = 11.65%
Stress	Increase =	20-1/2	9.43		
40 psi at	$\epsilon = 12.41\%$			95	11.66
_		Stress I	Decrease =	107	11.70
8635	12.61	40 psi at	€ = 9.43%	120	11.79
8725	12.73	-	-	135	11.86
8820	12.85	21	9.48	150	11.95
9095	13.09	22	9.54	165	12.01
9885	13.58	23	9.63	180	12.07
10015	13.66	24	9.73	205	12.19
		25	9.81	210	12.21
Stress	Increase =	27	9.97	213	12.22
	€ = 13.66%	28	10.05		
		30	10.20	Stress	Decrease =
10115	13.85	34	10.54	40 psi at	€ = 12.22%

TABLE III (Continued)

Time	True Strain	Time	True Strain	Time	True Strain
(Min.)	(%)	(Min.)	(%)	(Min.)	(%)
SAMPLE.	A-3(8) Contd.	120	9.29	6	7.00
		125	9.40	7	7.48
375	12.33	127	9.43	8	7.87
435	12.41			9	8.39
475	12.45	Stress	Decrease =	10	8.78
5 6 5	12.54	40 psi at	$\epsilon = 9.43\%$	11	9.15
				11-3/4	9.43
	NO. A-3(13)	128	9.4 6		
	ess = 675 psi	140	9.52		Decrease =
	Moisture	170	9.75	40 psi at	ϵ = 9.43%
Conter	nt = 26.16%	210	9.90		
_		235	10.03	12-1/2	9.60
1/2	. 34	245	10.06	14	9.73
1	• 99			15	9.83
1-1/2	1.79		Decrease =	16	9.96
2	2.47	40 psi at	ϵ = 10.06%	17	10.05
3	3.00	_		18	10.16
4	3.34	247	10.09	19	10.27
5	3.58	345	10.18	20	10.36
6	3.79	370	10.20	21	10.45
8	4.13	420	10.26	22	10.54
10	4.44	440	10.27	_	
12	4.69	_			Decrease =
15	5.02		Decrease =	40 psi at	$\epsilon = 10.54\%$
20	5.50	40 psi at	$\epsilon = 10.27\%$		
22	5.67			24	10.60
26	5. 98	525	10.27	25	10.62
30	6.25	590	10.28	26	10.66
33	6.42	1265	10.39	27	10.69
36	6.59	_		28	10.71
40	6.80		NO. $A-3(12)$	29	10.75
44	7.00		ess - 525 psi	30	10.77
48	7.17		Moisture	32	10.83
50	7.26	Content	t = 25.73%	35	10.94
58	7.57	• -		39	11.06
64	7.79	1/2		40	11.08
68	7.89	1	1.06	40-1/2	11.09
72	8.08	1-1/2			_
77	8.23	2	3.43		Decrease =
85	8.45	2-1/2		40 psi at	ϵ = 11.09%
95	8.69	3	4.76		
105	8.95	4	5.61	50 	11.11
116	9.20	5	6.37	55	11.13

TABLE III (Continued)

Time	True Strain	Time	True Strain	Time	True Strain
(Min.)	(%)	(Min.)	(%)	(Min.)	(%)
SAMPLE	A-3(12)Contd.	15	9.72	2980	13.90
		16	9.81	3940	13.93
90	11.38	17	9.90	4080	13.96
140	11.59	18	10.00	-	14.02
150	11.62	20	10.18		
158	11.65	22	10.39	Stress	Decrease =
		25	10.61		€ = 14.02%
Stress	Decrease =	28	10.81	•	
	€ = 11.65%	30	10.95	0	0
ro por do	22,0370	33	11.11	-	(14.02)
260	11.66	35	11.20	3	.03
440	11.73	39	11.43	8	.04
520	11.77	42	11.59	20	. 05
5 7 0	11.79	43	11.65	65	.11
1230	11.97	13	11.05	148	. 17
1230	11. / (Stress	Decrease =	170	. 19
SAMPLE	NO. A-3(6)		$\epsilon = 11.65\%$	855	.78
	ess = 400 psi	oo por at	(- 11.05/0	945	. 86
	Moisture	44	11.73	1070	. 98
		46	11.74	1070	1.01
Content = 25.62%		50	11.79	1001	(15.02)
1/2	.28	55	11.82		(13.02)
1	1.08	60	11.89	Strace	Increase =
1-1/2		70	11.99		t ϵ = 1.01%
2	3.25	95	12.23	_	$\begin{array}{cccccccccccccccccccccccccccccccccccc$
2-1/2		130	12.52		with respect
3	4.58	170	12.85		itial length.)
4	5. 48	180	12.92	to III	itiai length.
5	6.21	190	12.98	1093	1.08
	6.72	190	12. 90	1093	1.13
6		St	. D	1108	
7	7.25		Decrease =		1.26
8	7.67	ou psi at	ϵ = 12.98%	1128	1.46
9	8.07	300	12.00	1160	1.80
10	8.40	200	12.99	1175	1.93
11	8.76	360	13.10	1210	2.25
12	9.07	610	13.31		(16.25)
13	9.35	1180	13.78	Stress	Increase =
13+	9.43	1245	13.82		€ = 2.25%
Stress Decrease =		Stress Decrease =		(Corresponds to 16.25%	
	E = 9.43%		€ = 13.82%	_	pect to initial
Jo par at	C - 3. 43/0	Jo par at	C = 13.02/0		ength.)
14	9.61	1510	13.85	1213	2.41

TABLE III (Continued)

Time	True Strain	Time	True Strain	Time	True Strain
(Min.)	(%)	(Min.)	(%)	(Min.)	(%)
SAMPLE	A-3(6)Contd.				
1215	2.52	25	8.01	1/2	.71
1218	2.70	27	8.20	1	1.93
1220	2.80	30	8.46	1-1/2	3.46
1223	2.93	32	8.63	2	4.97
1226	3.09	35	8.87	2-1/2	6.39
1228	3.18	37	8.97	3	7.33
1230	3.26	40	9.15	4	8.65
	(17.28)	42	9.24	5	9.43
		44	9.35	6	10.46
Stress	Increase =	45+	9.43	6-1/2	10.78
30 psi at	ϵ = 3.26%			7	11.05
(Corresp	~	Stress	Decrease =		
•	with respect	30 psi at	$\epsilon = 9.43\%$	Stress	Decrease =
	al length.)	-		20 psi at	€ = 11.05%
	5 .	4 6	9.50	-	_
1231	3.50	50	9.52	7-1/2	11.10
12 3 2	3.69	60	9.63	8	11.19
1233	3.88	7 5	9.77	9	11.41
1234	4.04	90	9.90	10	11.68
1235	4. 23	130	10.17	11	11.89
	2. 20	150	10.28	12	12.14
SAMPLE	NO. A-3 (7)	170	10.40	13	12.34
Axial Stress = 350 psi		175	10.43	14	12.53
	Moisture				22.00
Content = 25.37%		Stress Decrease =		Stress Decrease =	
			€ = 10.43%		$\epsilon = 12.53\%$
1/	2 .36	•		•	
1	1.29	180	10.47	15	12.66
1-1/		330	10.51	16	12.69
2	2.68	395	10.55	17	12.73
3	3.41	540	10.61	18	12.78
4	3.92	1170	10.83	19	12.87
5	4. 36	1390	10.89	20	12.94
6	4.73	1580	10.91	21	13.01
7	5.06	1940	10.99	22	13.07
8	5. 36	2670	11.10	23	13.12
9	5.61	2810	11.13	24	13.18
10	5.84	2920	11.14	25	13.23
12	6.28	·	-	26	13.30
15	6.82	SAMPLE	NO. A-3(14)	27	13.40
18	7.25		ess = 260 psi		•
20	7.46	Final Moisture		Stress Decrease =	
23	7.83		t = 25.63%		€ = 13.40%

TABLE III (Continued)

	•		(00111111111111111111111111111111111111
Time	True Strain	Time	True Strain
(Min.)	(%)	(Min.)	(%)
SAMPLE	A-3(14)Contd.		16.81
		2126	17.14
28	13.42	a . •	
35	13.51		increase =
40	13.57	20 psi at	$\epsilon = 17.14\%$
50	13.69	2.24	
70	13.90	2126	17.21
140	14.43	2128	17.64
190	14.66	2130	18.01
		2132	18.38
Stress	Decrease =	2133	18.56
20 psi at	$\epsilon = 14.66\%$		
310	14.69		
370	14.71		
420	14.73		
1200	14.91		
1260	14.93		
1360	14.94		
1440	14.95		
1565	14.98		
1825	15.01		
Stress	Increase =		
20 psi at	$\epsilon = 15.01\%$		
1940	15.34		
2055	15.56		
2085	15.61		
Stress	Increase =		
20 psi at	€ 15.61%		
2090	15.72		
2095	15.82		
2100	15.89		
2105	15.97		
2110	16.06		
Stress	Increase =		
20 psi at	€ =16.06%		

16.49

2115



